# APPENDIX C
# PCB CONGENER AND COLLOID TRANSPORT MODEL

**CONTENTS** Page

## CONTENTS (Continued)

Page

### TABLES



### FIGURES

# APPENDIX C
# PCB CONGENER AND COLLOID TRANSPORT MODEL

## C.1.0 INTRODUCTION

### *C.1.1 Overview*

We developed ***RATLIM2D_PCB***, a new transient, two-dimensional PCB congener and colloid transport model of the shallow aquifer at the Kaiser Trentwood Facility. We developed the model to provide an important computational tool that we could use to analyze the October 2007 and April 2008 groundwater congener data sets and advance our understanding of the key PCB transport mechanisms at the Facility. In addition to congener data, the model uses many types of hydrogeologic and chemical data that have been collected during previous site investigations (e.g., soil organic carbon, hydraulic conductivity, hydraulic gradient, physical colloid characterization, etc.). ***RATLIM2D_PCB*** contains two modules—groundwater flow, and PCB congener and colloid transport models.

### *C.1.2 Flow Model*

The analytical flow model allows the incorporation of multiple boundary conditions representing various combinations of extraction and injection wells, no-flow boundaries, leaky-type (semi-pervious layer) boundaries such as rivers and lakes with complex geometries, and regional hydraulic gradients. The model is based on the superposition of Dupuit-Forchheimer solutions (Bear 1979) for flow to one or more wells and the effects of a regional hydraulic gradient. The geometry, bed-sediment conductance distributions and surface water elevation variations for rivers and lakes can be accurately represented because the model employs an iterative solution that dynamically links the hydraulic impacts of the water body on the aquifer.

### *C.1.3 PCB Congener Transport Model*

The PCB congener and colloid transport model is a sophisticated and comprehensive analysis tool that incorporates many chemical transport mechanisms. The model simulates the transport of all 209 PCB congeners simultaneously, both as aqueous phase (i.e., dissolved in groundwater) and colloidal phase (i.e., sorbed to mobile colloids flowing with the groundwater) fractions. Colloid filtration due to interactions with the porous media is also included. Because of the high groundwater velocities at the Facility, the model further incorporates rate-limited soil to groundwater chemical partitioning (non-equilibrium chemical sorption) and non-equilibrium groundwater to colloid PCB sorption mechanisms. We use the known chemical properties of PCB compounds to assign different soil/water partition coefficients to each congener based on published literature values and adjust these coefficients during model calibration.

A computationally efficient numerical algorithm is used to solve the governing solute transport equation. This solution technique, referred to as the Eulerian-Lagrangian method, uses different techniques to solve the advection and dispersion parts of the equation, thus avoiding numerical instabilities and excessive time-stepping constraints associated with traditional numerical methods. The backward method of characteristics (MOC) is used to solve the advection component. The MOC algorithm employs accurate and efficient semi-analytical pathline tracing methods developed by the USGS (Pollock 1988). Interpolation of concentrations at the feet of the characteristic lines, required as part of the MOC technique, is based on higher-order quadratic interpolation functions, thus avoiding the spurious numerical dispersion associated with linear interpolation methods. The alternating direction implicit (ADI) numerical technique is used to solve the dispersion part of the transport equation. Because the ADI method uses implicit time-stepping, much larger time steps can be used than with codes that solve the dispersion equation explicitly. The ability of ***RATLIM2D_PCB*** to handle large time steps is especially useful when simulating field-scale remediation systems due to the high velocities that naturally occur and the small grid cell sizes required around extraction wells.

The ADI method also minimizes computer memory requirements and simulation times because it only requires the formulation and solution of one-dimensional matrices. Another unique result of combining the Eulerian-Lagrangian technique with ADI methods is that the time-step size is not constrained by Courant number (related to velocity divided by cell size) restrictions, as is the case when ADI methods are used to solve the entire advection-dispersion equation.

## C.2.0 THEORY

### *C.2.1 Groundwater Flow*

The flow model is based on the superposition of Dupuit-Forchheimer solutions (Bear 1979) for flow to one or more wells in an unconfined aquifer and the effects of a regional hydraulic gradient. The solutions are also applicable to confined aquifers as long as the change in hydraulic head due to pumping or recharge is small compared to the saturated thickness.

## Hydraulic Head

The Dupuit-Forchheimer solution for the steady-state hydraulic head, *h*, in an unconfined aquifer with multiple ($N_w$) pumping or injection wells and vertical recharge rate, *I*, is given by (Bear 1979):

$$h_o^2 - h^2(x_i, y_i) = \sum_{j=1}^{N_w} \left[ \frac{Q_j}{\pi K} \ln\left(\frac{R_j}{r_{ij}}\right) - \frac{I\left(R_j^2 - r_{ij}^2\right)}{2K} + \frac{I r_{w_j}^2}{K} \ln\left(\frac{R_j}{r_{ij}}\right) \right] \qquad (2\text{-}1)$$

where:

$h_o$ is the initial hydraulic head without pumping wells or recharge;
($x_i$,$y_i$) are the horizontal coordinates of the model grid;
*Q* is the pumping rate (positive for groundwater extraction, negative for injection);
*K* is the hydraulic conductivity of the aquifer;
*R* is the radius of influence of the pumping well;
*r* is the radial distance from the well to a point ($x_i$,$y_i$) on the model grid;
$r_w$ is the radius of the pumping well; and

$$r_{ij} = \sqrt{\left(x_i - x_{w_j}\right)^2 + \left(y_i - y_{w_j}\right)^2}$$

$$R_j = \sqrt{r_{w_j}^2 + \frac{Q}{\pi I}}$$

After rearranging Equation (2-1), the expression for hydraulic head, *h*, is:

$$h(x_i, y_i) = \sqrt{ h_o^2 - \sum_{j=1}^{N_w} \left\{ \left[ \frac{Q_j}{\pi K} + \frac{I r_{w_j}^2}{K} \right] \ln\left(\frac{R_j}{r_{ij}}\right) - \frac{I}{2K}\left(R_j^2 - r_{ij}^2\right) \right\} } \qquad (2\text{-}2)$$

Equation (2-2) can be further modified to add in the effects of a regional hydraulic gradient, $i_R$, which is defined as positive for decreasing hydraulic head in the direction of the regional flow, defined as $\theta_R$ (Figure C-1). It is also useful to establish a datum by defining a reference head, $h_{ref}$, that represents a known water table elevation at a point $(x_o, y_o)$. The equation for the hydraulic head, *H*, referenced to a datum is then defined as:

$$H(x_i, y_i) = h(x_i, y_i) + (h_{ref} - h_o) - i_R\left[\left(x_i - x_o\right)\cos\left(\theta_R\right) + \left(y_i - y_o\right)\sin\left(\theta_R\right)\right] \qquad (2\text{-}3)$$



**Figure 2-1**

## Pore Velocities

The *x*- and *y*-direction Darcy pore velocities, *u and v*, are defined as:

$$u = \frac{-K}{n_e}\frac{\partial H}{\partial x}; \quad v = \frac{-K}{n_e}\frac{\partial H}{\partial y} \qquad (2\text{-}4)$$

where:

$n_e$ is the effective soil porosity.

Analytical solutions for the pore velocities can be derived from Equations (2-3) and (2-4) as follows. First, define an auxiliary variable $\omega$:

$$\omega = h_o^2 - \sum_{j=1}^{N_w} \left\{ \left( \frac{Q_j}{\pi K} + \frac{I\, r_{w_j}^2}{K} \right) \ln\left( \frac{R_j}{r_{ij}} \right) - \frac{I}{2K}\left( R_j^2 - r_{ij}^2 \right) \right\} \qquad (2\text{-}5)$$

Then, by definition $h = \sqrt{\omega}$ and

$$\frac{\partial H}{\partial x} = \frac{1}{2\sqrt{\omega}}\frac{\partial \omega}{\partial x} - i_R \cos(\theta_R) \qquad (2\text{-}6)$$

where:

$$\frac{\partial \omega}{\partial x} = \frac{1}{\pi K}\sum_{j=1}^{N_w} \frac{1}{r_{ij}}\frac{\partial r_{ij}}{\partial x}\left[ Q_j + \pi I \left( r_{w_j}^2 - r_{ij}^2 \right) \right]$$

and

$$\frac{\partial r_{ij}}{\partial x} = \frac{x_i - x_{w_j}}{r_{ij}}$$

which gives:

$$u(x_i, y_i) = \frac{-1}{2\pi n_e\, h(x_i, y_i)} \sum_{j=1}^{N_w} \left\{ \frac{1}{r_{ij}^2}\left( x_i - x_{w_j} \right)\left[ Q_j + \pi I \left( r_{w_j}^2 - r_{ij}^2 \right) \right] \right\} + \frac{K\, i_R}{n_e}\cos(\theta_R) \qquad (2\text{-}7)$$

Following a similar derivation for the *y*-direction pore velocity, the following result is obtained:

$$v(x_i, y_i) = \frac{-1}{2\pi n_e\, h(x_i, y_i)} \sum_{j=1}^{N_w} \left\{ \frac{1}{r_{ij}^2}\left( y_i - y_{w_j} \right)\left[ Q_j + \pi I \left( r_{w_j}^2 - r_{ij}^2 \right) \right] \right\} + \frac{K\, i_R}{n_e}\sin(\theta_R) \qquad (2\text{-}8)$$

## Boundary Conditions

### *Rivers and Lakes (Leaky-Type Boundaries)*

Rivers and lakes can easily be added by defining the water body geometry and inputting data for the river/lake stage, $\phi_o$; the bed sediment hydraulic conductivity, $k_{RL}$; and the bed sediment thickness, $\Delta z_{RL}$. The total vertical flow rate, $Q_{RL}$, entering the aquifer from any river or lake cell in the grid system is equal to:

$$Q_{RL} = k_{RL} \frac{\phi_o - H}{\Delta z_{RL}} \Delta x \, \Delta y \qquad (2\text{-}9)$$

where:

$\Delta x$ and $\Delta y$ are the grid cell dimensions; and
$k_{RL} / \Delta z_{RL}$ is the river/lake bed conductance.

The aquifer inflows or losses due to lakes and rivers are incorporated into Equation (2-2) as additional wells. Because the hydraulic head in the aquifer, $H$, is dependent on the flow from the water body, $Q_{RL}$, an iterative solution procedure is employed. First, $H(x,y)$ is computed from Equation (2-3) without river or lake boundary conditions; this initial estimate is then used to calculate $Q_{RL}$ at each river/lake cell. Second, Equations (2-2) and (2-3) are used to update the $H(x,y)$ distribution based in the initial $Q_{RL}$ estimates. The process of updating $Q_{RL}$ and $H$ is repeated until the maximum change in $H$ is less than a user-specified head tolerance, $\Delta H$ (e.g., $\Delta H$ = 0.001 foot).

For a lake, one bed conductance and water surface elevation (i.e., stage), $\phi_o$, are specified. For a river, values of conductance and stage are specified at each of the construction points that the user selects to define the river geometry. The program linearly interpolates between construction points to establish conductance and stage values at grid cells that intercept river segments.

### *Constant-Head Boundary*

Constant-head boundaries or regions can be created using the river/lake option and specifying a large bed conductance (e.g., $k_{RL} = K$) so that a good hydraulic connection between the water body and aquifer is established. To avoid convergence problems with the iterative solution scheme described above, we recommend that the river/lake bed hydraulic conductivity, $k_{RL}$, not exceed the hydraulic conductivity of the aquifer, $K$.

#### *No-Flow Boundary*

The code allows the optional specification of one linear, no-flow boundary (e.g., Figure C-1). Cells located within this area are set inactive for flow and contaminant transport simulations. If a regional gradient is specified, the regional flow direction is automatically changed so that it is parallel to the no-flow boundary. For each pumping/injection well and each river/lake cell, the flow code defines image wells on the opposite side of the no-flow boundary to create the desired effect of no groundwater flux across the boundary.

### *C.2.2 PCB and Colloid Transport*

#### Governing Conservation of Mass Equation—Aqueous Phase PCBs

The depth-averaged, two-dimensional transport equation governing the conservation of aqueous phase PCB in groundwater and soil with non-equilibrium sorption is (van Genuchten and Wagenet 1989; Bentley and Pinder 1992; Culver et al., 1997):

$$b\,\frac{\partial c_{w_i}}{\partial t} + bu\,\frac{\partial c_{w_i}}{\partial x} + bv\,\frac{\partial c_{w_i}}{\partial y} = \frac{\partial}{\partial x}\left[bD_{xx}\frac{\partial c_{w_i}}{\partial x} + bD_{xy}\frac{\partial c_{w_i}}{\partial y}\right] + \frac{\partial}{\partial y}\left[bD_{yx}\frac{\partial c_{w_i}}{\partial x} + bD_{yy}\frac{\partial c_{w_i}}{\partial y}\right]$$

$$-\,b\,\frac{\rho_b}{n}\,\alpha\left[k_{d_i}\,c_{w_i} - s_{2_i}\right] - b\,\rho_o^*\,\alpha_{coll}\left[(k_d)_{coll_i}\,c_{w_i} - c_{o_i}\right] - b\,\frac{\sigma_o}{n}\,\alpha_{coll}\left[(k_d)_{coll_i}\,c_{w_i} - S_{\sigma_i}\right]$$

$$-\,\frac{I}{n}\,(c_{w_i} - c_{w_{\inf_i}}) \qquad \text{(2-10)}$$

where:

*b(x,y)* is the saturated thickness (length) of the aquifer;
$c_{w_i}(x, y, t)$ is the aqueous phase PCB concentration (mass/volume) for congener "*i*" (i=1, $N_{cong}$);
$N_{cong}$ is the number of congeners;
*t* is time;
*u* and *v* are the *x*- and *y*-direction pore velocities (length/time), respectively;
$D_{ij}$ is the dispersion coefficient tensor (length$^2$/time);
$\rho_b$ is the soil bulk density (mass/volume);
$k_{d_i}$ is the soil-water partition coefficient for congener "*i*" (volume/mass);
*n* is the soil porosity (dimensionless);
$s_{2_i}$ is the PCB congener concentration in the soil (mass congener/mass soil);

$\alpha$ is the first-order kinetic rate coefficient for PCB transfer between the soil and pore water phases (1/time);
$\rho_o^*$ is the mobile colloid (i.e., colloid mass that has not been filtered by the aquifer) concentration (mass mobile colloids/volume groundwater);
$\alpha_{coll}$ is the first-order kinetic rate coefficient for PCB transfer between the colloid and pore-water phases (1/time);
$(k_d)_{coll_i}$ is the colloid-water partition coefficient for congener "*i*" (volume/mass);
$c_{o_i}$ is the mobile colloid PCB concentration for congener "*i*" (mass congener/mass mobile colloid);
$\sigma_o$ is the immobile (i.e., colloids mass that has been filtered from the mobile groundwater) colloid concentration (mass immobile colloids/volume groundwater);
$S_{\sigma_i}$ is the immobile colloid PCB concentration for congener "*i*" (mass congener/mass immobile colloid);
I is the groundwater recharge rate; and
$c_{w_{\inf_i}}$ is the concentration of PCB congener "*i*" in the infiltrating water.

The hydrodynamic dispersion coefficients, $D_{ij}$ are defined as follows:

$$D_{xx} = a_T V_o + (a_L - a_T)\frac{u^2}{V_o} + \tilde{D}_m$$

$$D_{xy} = D_{yx} = (a_L - a_T)\frac{uv}{V_o} \qquad (2\text{-}11)$$

$$D_{yy} = a_T V_o + (a_L - a_T)\frac{v^2}{V_o} + \tilde{D}_m$$

where:

$a_L$ is the longitudinal dispersivity (length);
$a_T$ is the transverse dispersivity (length);
$\tilde{D}_m$ is the effective molecular diffusion coefficient in a porous medium ($\tilde{D}_m = \tau D_m$);
$\tau$ is tortuosity;
$D_m$ is the molecular diffusion coefficient in free water; and
$V_o = \sqrt{u^2 + v^2}$ .

## Governing Conservation of Mass Equation—Mobile Colloids

$$b \frac{\partial \rho_o^*}{\partial t} + bu \frac{\partial \rho_o^*}{\partial x} + bv \frac{\partial \rho_o^*}{\partial y} = \frac{\partial}{\partial x}\left[ bD_{xx} \frac{\partial \rho_o^*}{\partial x} + bD_{xy} \frac{\partial \rho_o^*}{\partial y} \right] + \frac{\partial}{\partial y}\left[ bD_{yx} \frac{\partial \rho_o^*}{\partial x} + bD_{yy} \frac{\partial \rho_o^*}{\partial y} \right]$$

$$- b\, \lambda_o\, \rho_o^* - \frac{I}{n} (\rho_o^* - \rho_{o_{\inf}}^*) \qquad (2\text{-}12)$$

where:

$\lambda_o = f_c\, u$ is the mobile colloid reduction (loss) coefficient (1/time) due to colloid filtration by the aquifer matrix;
$f_c$ is the colloid filtration coefficient (1/length); and
$\rho_{o_{\inf}}^*$ is the colloid concentration in infiltrating water.

## Governing Conservation of Mass Equation—Immobile Colloid Concentration

$$\frac{\partial \sigma_o}{\partial t} = \lambda_o\, n\, \rho_o^* \qquad (2\text{-}13)$$

## Governing Conservation of Mass Equation—PCBs in Soil

$$\frac{\partial s_{2_i}}{\partial t} = \alpha \left[ k_{d_i}\, c_{w_i} - s_{2_i} \right] \qquad (2\text{-}14)$$

## Governing Conservation of Mass Equation—PCBs Adsorbed to Immobile Colloids

$$\frac{\partial S_{\sigma_i}}{\partial t} = \frac{\lambda_o\, n\, \rho_o^*\, c_{o_i}}{\sigma_o} + \alpha_{coll} \left[ (k_d)_{coll_i}\, c_{w_i} - S_{\sigma_i} \right] \qquad (2\text{-}15)$$

### Governing Conservation of Mass Equation—PCBs Adsorbed to Mobile Colloids

$$b \frac{\partial c_{o_i}}{\partial t} + bu \frac{\partial c_{o_i}}{\partial x} + bv \frac{\partial c_{o_i}}{\partial y} = \frac{\partial}{\partial x}\left[bD_{xx}\frac{\partial c_{o_i}}{\partial x} + bD_{xy}\frac{\partial c_{o_i}}{\partial y}\right] + \frac{\partial}{\partial y}\left[bD_{yx}\frac{\partial c_{o_i}}{\partial x} + bD_{yy}\frac{\partial c_{o_i}}{\partial y}\right]$$

$$+ \; b \; \alpha_{coll}\left[(k_d)_{coll_i} \; c_{w_i} - c_{o_i}\right] - \; b \; \lambda_o \, c_{o_i} \; - \; \frac{I}{\rho_o^* \, n}\,[c_{o_i}\,\rho_o^* \; - \; (c_{o_i}\,\rho_o^*)_{\inf}\,] \qquad (2\text{-}16)$$

### Governing Conservation of Mass Equation—Total Mobile PCB Congener

$$c_i^* = c_{w_i} + \rho_o^* \, c_{o_i} \qquad (2-17)$$

where:

$c_i^*$ is the total mobile concentration (mass/volume) of congener "*i*" in groundwater (i.e., aqueous phase PCBs + congener mass adsorbed to mobile colloids).

## *C.2.3 Numerical Solution*

### Solution Approach

The conservation of mass equations for aqueous phase and colloidal PCBs (each congener) and mobile colloids are solved in three separate steps based on a time-derivative operator splitting technique. We use the Eulerian-Lagrangian method (Baptista 1987) to solve the advection and dispersion terms in the first two steps. In the third step, we use a fourth-order accurate Runge-Kutta scheme (Press et al., 1986) to implicitly solve the system of first-order ordinary differential equations that define the remaining conservation of mass equations.

By using finite-difference approximations to the time derivative and defining an auxiliary concentration variable, ĉ (i.e., intermediate concentrations that are computed during the process of advancing the solution from the old time level "*n*" to the new time level "*n+1*"), the advection and dispersion terms in Equations 2-10, 2-12, and 2-16 can be decomposed into two equations, as follow (Baptista 1987):

### *Advection*

$$\frac{\hat{c}^n - c^n}{\Delta t} + \left(u \frac{\partial c}{\partial x}\right)^n + \left(v \frac{\partial c}{\partial y}\right)^n = 0 \qquad (2\text{-}18)$$

### *Dispersion*

$$b \frac{c^{n+1} - \hat{c}^n}{\Delta t} = \frac{\partial}{\partial x}\left[bD_{xx}\frac{\partial c}{\partial x} + bD_{xy}\frac{\partial c}{\partial y}\right]^{n+1} + \frac{\partial}{\partial y}\left[bD_{yx}\frac{\partial c}{\partial x} + bD_{yy}\frac{\partial c}{\partial y}\right]^{n+1}$$

(2-19)

## Advection Equation

The solution of the advection portion of the transport equation by the reverse or backward method of characteristics is based on the fact that concentration in a parcel of water does not change as it moves from point to point. Therefore, computing water concentrations, $\hat{c}^n$, at a new time level due to advection involves two main tasks: (1) back-tracking (reverse pathline tracing) of particles along characteristic lines for a time period, $\Delta t$, starting from each node on the finite element grid; and (2) spatial interpolation using neighboring values of $c^n$ to determine the concentration at the endpoint (foot) of the characteristic line (Figure C-2).

Two-dimensional particle tracking is performed using the semi-analytical method developed by Pollock (1988). Spatial interpolation to compute the concentration, $\hat{c}$, is based on a bi-quadratic shape function, $N_i(x,y)$, and the concentrations, $c_i$, for the closest set of nine nodes surrounding the element that contains the foot of the characteristic line:

$$\hat{c} = \sum_{i=1}^{9} N_i(x,y)\, c_i \qquad (2\text{-}20)$$

$$N_1(x) = \frac{(x-x_2)(x-x_3)}{(x_1-x_2)(x_1-x_3)} \qquad N_1(y) = \frac{(y-y_2)(y-y_3)}{(y_1-y_2)(y_1-y_3)}$$

$$N_2(x) = \frac{(x-x_1)(x-x_3)}{(x_2-x_1)(x_2-x_3)} \qquad N_2(y) = \frac{(y-y_1)(y-y_3)}{(y_2-y_1)(y_2-y_3)}$$

$$N_3(x) = \frac{(x-x_1)(x-x_2)}{(x_3-x_1)(x_3-x_2)} \qquad N_3(y) = \frac{(y-y_1)(y-y_2)}{(y_3-y_1)(y_3-y_2)}$$

$$N_1(x,y) = N_1(x)\,N_1(y) \qquad N_4(x,y) = N_3(x)\,N_2(y) \qquad N_7(x,y) = N_1(x)\,N_3(y)$$

$$N_2(x,y) = N_2(x)\,N_1(y) \qquad N_5(x,y) = N_3(x)\,N_3(y) \qquad N_8(x,y) = N_1(x)\,N_2(y)$$

$$N_3(x,y) = N_3(x)\,N_1(y) \qquad N_6(x,y) = N_2(x)\,N_3(y) \qquad N_9(x,y) = N_2(x)\,N_2(y)$$

Quadratic interpolation functions are computationally efficient and minimize numerical damping (Baptista 1987). However, higher-order interpolation methods can introduce numerical oscillations (e.g., negative concentrations) near steep concentration fronts. If such oscillations are detected, linear interpolation is used for that specific node. This mixed quadratic/linear technique was developed by Healy and Russell (1989) and eliminates oscillations while adding only minimal and localized numerical dispersion.

## Dispersion Equation

The ADI method of Douglas (1962) is used to solve Equation (2-19). The overall approach is similar to method developed by Daus and Frind (1985) except that they adopted the Peaceman-Rachford ADI technique and solved both the advection and dispersion terms. The numerical approximation of the two-dimensional dispersion equation is handled in two separate steps consisting of consecutive one-dimensional, implicit solutions in the *x*- and *y*-directions (Figure C-3):

**Step 1**

$$\frac{c^{*\,n+1} - \hat{c}^{\,n}}{\Delta t} = \tfrac{1}{2}\left(L_{yx} + L_{xx}\right)\left(c^{*\,n+1} + \hat{c}^{\,n}\right) + \left(L_{xy} + L_{yy}\right)\hat{c}^{\,n} \qquad (2-21a)$$

**Step 2**

$$\frac{c^{n+1} - c^{*\,n+1}}{\Delta t} = \tfrac{1}{2}\left(L_{xy} + L_{yy}\right)\left(c^{n+1} - \hat{c}^{\,n}\right) \qquad (2-21b)$$

where the subscripts in the differential operator $L_{ij}$ indicate the spatial dependence and the solution is second-order accurate in space and time (Lapidus and Pinder 1982). The second-order temporal approximation requires that the terms $L_{ij}\,\hat{c}^{\,n}$ be evaluated at the foot of the characteristic line. The spatial variations of concentration are defined as follows:

**Step 1 (x-direction)**

$$c \cong N_1(x)c_1 + N_2(x)c_2$$

$$N_1(x) = \frac{x_2 - x}{x_2 - x_1} \qquad N_2(x) = \frac{x - x_1}{x_2 - x_1} \qquad (2\text{-}22a)$$

**Step 2 (y-direction)**

$$c \cong N_1(y)c_1 + N_2(y)c_2 \qquad \text{(2-22b)}$$

$$N_1(y) = \frac{y_2 - y}{y_2 - y_1} \qquad N_2(y) = \frac{y - y_1}{y_2 - y_1}$$

The Galerkin finite element method (Huebner 1975) is applied in each direction, as follows:

**Step 1**

$$\sum_{x-dir.\ elements} \int_x\int_y \left\{ \frac{1}{2}\left(\frac{\partial}{\partial x}\left[bD_{xx}\frac{\partial c^*}{\partial x}\right] + \frac{\partial}{\partial y}\left[bD_{yx}\frac{\partial c^*}{\partial x}\right]\right)^{n+1} + \frac{1}{2}\left(\frac{\partial}{\partial x}\left[bD_{xx}\frac{\partial \hat{c}}{\partial x}\right] + \frac{\partial}{\partial y}\left[bD_{yx}\frac{\partial \hat{c}}{\partial x}\right]\right)^{n}\right.$$

$$\left. + \left(\frac{\partial}{\partial y}\left[bD_{yy}\frac{\partial \hat{c}}{\partial y}\right] + \frac{\partial}{\partial x}\left[bD_{xy}\frac{\partial \hat{c}}{\partial y}\right]\right)^{n} - b\left(\frac{c^{*\,n+1} - \hat{c}^{n}}{\Delta t}\right)\right\} N_i\ (x)\ dy\ dx = 0 \qquad ,i = 1,2 \qquad \text{(2-23a)}$$

**Step 2**

$$\sum_{y-dir.\ elements} \int_y\int_x \left\{ \frac{1}{2}\left(\frac{\partial}{\partial y}\left[bD_{yy}\frac{\partial c}{\partial y}\right] + \frac{\partial}{\partial x}\left[bD_{xy}\frac{\partial c}{\partial y}\right]\right)^{n+1} - \frac{1}{2}\left(\frac{\partial}{\partial y}\left[bD_{yy}\frac{\partial \hat{c}}{\partial y}\right] + \frac{\partial}{\partial x}\left[bD_{xy}\frac{\partial \hat{c}}{\partial y}\right]\right)^{n}\right.$$

$$\left. - b\left(\frac{c^{n+1} - c^{*\,n+1}}{\Delta t}\right)\right\} N_i\ (y)\ dx\ dy = 0 \qquad i = 1,2 \qquad \text{(2-23b)}$$

First, integrate Equations (2-23a and 2-23b) across the explicit directions:

**Step 1**

$$\sum_{x-dir.\ elements} \left\{ \int_x \frac{1}{2}\Delta y \left(\frac{\partial}{\partial x}\left[bD_{xx}\frac{\partial c^*}{\partial x}\right]\right)^{n+1} N_i(x)\ dx + \int_x \frac{1}{2}\left(\left. bD_{yx}\frac{\partial c^*}{\partial x}\right|_{y_2} - \left. bD_{yx}\frac{\partial c^*}{\partial x}\right|_{y_1}\right)^{n+1} N_i(x)\ dx\right.$$

$$+ \int_x \frac{1}{2}\Delta y\left(\frac{\partial}{\partial x}\left[bD_{xx}\frac{\partial \hat{c}}{\partial x}\right]\right)^{n} N_i(x)\ dx + \int_x \frac{1}{2}\Delta y\left(\frac{\partial}{\partial y}\left[bD_{yx}\frac{\partial \hat{c}}{\partial x}\right]\right)^{n} N_i(x)\ dx$$

$$+ \int_x \Delta y\left(\frac{\partial}{\partial y}\left[bD_{yy}\frac{\partial \hat{c}}{\partial y}\right]\right)^{n} N_i(x)\ dx + \int_x \Delta y\left(\frac{\partial}{\partial x}\left[bD_{xy}\frac{\partial \hat{c}}{\partial y}\right]\right)^{n} N_i(x)\ dx$$

$$- \int_x \Delta y\, b\, \frac{1}{\Delta t}\, c^{*\, n+1}\, N_i(x)\, dx \;+\; \int_x \Delta y\, b\, \frac{1}{\Delta t}\, \hat{c}\, N_i(x)\, dx \Bigg\} \;=\; 0 \qquad i = 1,2 \qquad \text{(2-24a)}$$

**Step 2**

$$\sum_{y-dir.\ elements} \Bigg\{ \int_y \frac{1}{2}\, \Delta x \left( \frac{\partial}{\partial y}\left[ bD_{yy} \frac{\partial c}{\partial y} \right] \right)^{n+1} N_i(y)\, dy \;+\; \int_y \frac{1}{2} \left[ \left( bD_{xy} \frac{\partial c}{\partial y} \right)\bigg|_{x_2} - \left( bD_{xy} \frac{\partial c}{\partial y} \right)\bigg|_{x_1} \right]^{n+1} N_i(y)\, dy$$

$$- \int_y \frac{1}{2}\, \Delta x \left( \frac{\partial}{\partial y}\left[ bD_{yy} \frac{\partial \hat{c}}{\partial y} \right] \right)^{n} N_i(y)\, dy \;-\; \int_y \frac{1}{2}\, \Delta x \left( \frac{\partial}{\partial x}\left[ bD_{xy} \frac{\partial \hat{c}}{\partial y} \right] \right)^{n} N_i(y)\, dy \qquad \text{(2-24b)}$$

$$- \int_y \Delta x\, b\, \frac{1}{\Delta t}\, c^{n+1}\, N_i(y)\, dy \;+\; \int_y \Delta x\, b\, \frac{1}{\Delta t}\, c^{*\, n+1}\, N_i(y)\, dy \Bigg\} \;=\; 0 \qquad i = 1,2$$

Next we integrate the equations in the implicit directions using integration by parts and assuming the resulting dispersive flux terms at the boundaries are zero. $b$ and $D_{ij}$ are assumed to be constant across an element.

**Step 1**

$$\sum_{x-dir.\ elements} \Bigg\{ - \langle \mathbf{c} \rangle^{n+1} \Delta y/2 \int_x D_{xx} b \frac{\partial\, \mathbf{N_j}\, \mathbf{N_i}}{\partial x\, \partial x}\, dx \;+\; \frac{1}{2} \left[ \left( bD_{yx} \frac{\partial c^*}{\partial x} \right)\bigg|_{y_2} - \left( bD_{yx} \frac{\partial c^*}{\partial x} \right)\bigg|_{y_1} \right]^{n+1} \begin{pmatrix} \Delta x/2 \\ \Delta x/2 \end{pmatrix}$$

$$+ \left\langle \frac{\partial}{\partial x}\left( \hat{\mathbf{b}}\, \hat{\mathbf{D}}_{\mathbf{xx}} \frac{\partial\, \hat{\mathbf{c}}}{\partial x} \right) \right\rangle^{n} \Delta y/2 \left[ \mathbf{G'_X} \right] \;+\; \left\langle \frac{\partial}{\partial y}\left( \hat{\mathbf{b}}\, \hat{\mathbf{D}}_{\mathbf{yx}} \frac{\partial\, \hat{\mathbf{c}}}{\partial x} \right) \right\rangle^{n} \Delta y/2 \left[ \mathbf{G'_X} \right]$$

$$+ \left\langle \frac{\partial}{\partial y}\left( \hat{\mathbf{b}}\, \hat{\mathbf{D}}_{\mathbf{yy}} \frac{\partial\, \hat{\mathbf{c}}}{\partial y} \right) \right\rangle^{n} \Delta y \left[ \mathbf{G'_X} \right] \;+\; \left\langle \frac{\partial}{\partial x}\left( \hat{\mathbf{b}}\, \hat{\mathbf{D}}_{\mathbf{xy}} \frac{\partial\, \hat{\mathbf{c}}}{\partial y} \right) \right\rangle^{n} \Delta y \left[ \mathbf{G'_X} \right] \qquad \text{(2-25a)}$$

**Step 2**

$$\sum_{y-dir.\ elements} \Bigg\{ - \langle \mathbf{c} \rangle^{n+1} \Delta x/2 \int_y D_{yy} b \frac{\partial\, \mathbf{N_j}\, \mathbf{N_i}}{\partial y\, \partial y}\, dy \;+\; \frac{1}{2} \left[ \left( bD_{xy} \frac{\partial c}{\partial y} \right)\bigg|_{x_2} - \left( bD_{xy} \frac{\partial c}{\partial y} \right)\bigg|_{x_1} \right]^{n+1} \begin{pmatrix} \Delta y/2 \\ \Delta y/2 \end{pmatrix}$$

$$- \left\langle \frac{\partial}{\partial y}\left( \hat{\mathbf{b}}\, \hat{\mathbf{D}}_{\mathbf{yy}} \frac{\partial\, \hat{\mathbf{c}}}{\partial y} \right) \right\rangle^{n} \Delta x/2 \left[ \mathbf{G'_y} \right] \;-\; \left\langle \frac{\partial}{\partial x}\left( \hat{\mathbf{b}}\, \hat{\mathbf{D}}_{\mathbf{xy}} \frac{\partial\, \hat{\mathbf{c}}}{\partial y} \right) \right\rangle^{n} \Delta x/2 \left[ \mathbf{G'_y} \right] \qquad \text{(2-25b)}$$

$$- \left\langle \mathbf{c} \right\rangle^{n+1} \Delta x\, b \;/ \Delta t \left[ \mathbf{G}_{\mathbf{y}}^{'} \right] \;+\; \left\langle \mathbf{b}\, \mathbf{c}^{*} \right\rangle^{n+1} \Delta x \;/ \Delta t \left[ \mathbf{G}_{\mathbf{y}}^{'} \right] \;=\; 0$$

where:

$$\int_x \frac{\partial\, \mathbf{N_j}\; \partial\, \mathbf{N_i}}{\partial\, x\, \partial\, x}\, dx \;=\; \frac{1}{\Delta\, x} \begin{bmatrix} +1 & -1 \\ -1 & +1 \end{bmatrix} \qquad \int_y \frac{\partial\, \mathbf{N_j}\; \partial\, \mathbf{N_i}}{\partial\, y\, \partial\, y}\, dy \;=\; \frac{1}{\Delta\, y} \begin{bmatrix} +1 & -1 \\ -1 & +1 \end{bmatrix}$$

$$\int_x \mathbf{N_j N_i}\; dx \;=\; \frac{1}{\Delta\, x^2} \begin{bmatrix} \left(x_2^3 - x_1^3\right)/3 \,+\, x_2 x_1^2 \,-\, x_2^2 x_1 & \left(x_2^3 - x_1^3\right)/6 \,-\, x_1 x_2^2/2 \,+\, x_2 x_1^2/2 \\ \left(x_2^3 - x_1^3\right)/6 \,-\, x_1 x_2^2/2 \,+\, x_2 x_1^2/2 & \left(x_2^3 - x_1^3\right)/3 \,+\, x_1^2 x_2 \,-\, x_1 x_2^2 \end{bmatrix}$$

$$\int_y \mathbf{N_j N_i}\; dy \;=\; \frac{1}{\Delta\, y^2} \begin{bmatrix} \left(y_2^3 - y_1^3\right)/3 \,+\, y_2 y_1^2 \,-\, y_2^2 y_1 & \left(y_2^3 - y_1^3\right)/6 \,-\, y_1 y_2^2/2 \,+\, y_2 y_1^2/2 \\ \left(y_2^3 - y_1^3\right)/6 \,-\, y_1 y_2^2/2 \,+\, y_2 y_1^2/2 & \left(y_2^3 - y_1^3\right)/3 \,+\, y_1^2 y_2 \,-\, y_1 y_2^2 \end{bmatrix}$$

Rearranging Equations (2-25a and 2-25b) gives:

**Step 1**

$$\sum_{x-dir.\ elements} \Bigg\{ \left\langle \mathbf{c}^{*} \right\rangle^{n+1} \left( \frac{-\Delta\, y}{2}\; \frac{\overline{bD_{xx}}}{\Delta\, x} \begin{bmatrix} +1 & -1 \\ -1 & +1 \end{bmatrix} \;-\; \Delta\, y\, \bar{b}\; \frac{1}{\Delta\, t} \left[ \mathbf{G}_{\mathbf{x}}^{'} \right] \right) \;+\; \frac{1}{4} \left\langle \frac{\Delta\, x}{\Delta\, x} \right\rangle \left[ bD_{yx} \left. \frac{\partial\, c^{*}}{\partial\, x} \right|_{y_2} - \; bD_{yx} \left. \frac{\partial\, c^{*}}{\partial\, x} \right|_{y_1} \right]^{n+1}$$

$$+ \left[ \mathbf{G}_{\mathbf{x}}^{'} \right] \Delta\, y \left( \frac{1}{2} \left\langle \frac{\partial}{\partial\, x} \left( \hat{b}\hat{D}_{xx} \frac{\partial\, \hat{c}}{\partial\, x} \right) \right\rangle^{n} \;+\; \frac{1}{2} \left\langle \frac{\partial}{\partial\, y} \left( \hat{b}\hat{D}_{yx} \frac{\partial\, \hat{c}}{\partial\, x} \right) \right\rangle^{n} \right. \tag{2-26a}$$

$$\left. + \left\langle \frac{\partial}{\partial\, y} \left( \hat{b}\hat{D}_{yy} \frac{\partial\, \hat{c}}{\partial\, y} \right) \right\rangle^{n} \;+\; \left\langle \frac{\partial}{\partial\, x} \left( \hat{b}\hat{D}_{xy} \frac{\partial\, \hat{c}}{\partial\, y} \right) \right\rangle^{n} \;+\; \left\langle \hat{b}\; \hat{c} \right\rangle^{n} \; \frac{1}{\Delta\, t} \right) \Bigg\} \;=\; 0$$

**Step 2**

$$\sum_{y-dir.\ elements} \Bigg\{ \left\langle \mathbf{c} \right\rangle^{n+1} \left( \frac{-\Delta\, x}{2}\; \frac{\overline{bD_{yy}}}{\Delta\, y} \begin{bmatrix} +1 & -1 \\ -1 & +1 \end{bmatrix} \;-\; \Delta\, x\, \bar{b}\; \frac{1}{\Delta\, t} \left[ \mathbf{G}_{\mathbf{y}}^{'} \right] \right) \;+\; \frac{1}{4} \left\langle \frac{\Delta\, y}{\Delta\, y} \right\rangle \left[ bD_{xy} \left. \frac{\partial\, c}{\partial\, y} \right|_{x_2} - \; bD_{xy} \left. \frac{\partial\, c}{\partial\, y} \right|_{x_1} \right]^{n+1}$$

$$+ \left[ \mathbf{G}_{\mathbf{y}}^{'} \right] \Delta\, x \left( \;-\; \frac{1}{2} \left\langle \frac{\partial}{\partial\, y} \left( \hat{b}\hat{D}_{yy} \frac{\partial\, \hat{c}}{\partial\, y} \right) \right\rangle^{n} \;-\; \frac{1}{2} \left\langle \frac{\partial}{\partial\, x} \left( \hat{b}\hat{D}_{xy} \frac{\partial\, \hat{c}}{\partial\, y} \right) \right\rangle^{n} \;+ \left\langle b\; c^{*} \right\rangle^{n+1} \; \frac{1}{\Delta\, t} \right) \Bigg\} \;=\; 0 \tag{2-26b}$$

### *Final Matrix Equations*

**Step 1**

$$\left[\mathbf{A_x}\right]\left\langle \mathbf{c}^{*}\right\rangle^{n+1} = \left\langle \overset{*}{\mathbf{F}}_{\mathbf{yx}}\right\rangle^{n+1} + \left\langle \hat{\mathbf{F}}_{\mathbf{x}}\right\rangle^{n} \qquad (2-27a)$$

**Step 2**

$$\left[\mathbf{A_y}\right]\left\langle \mathbf{c}\right\rangle^{n+1} = \left\langle \mathbf{F_{xy}}\right\rangle^{n+1} + \left\langle \hat{\mathbf{F}}_{\mathbf{y}}\right\rangle^{n} + \left\langle \overset{*}{\mathbf{F}}\right\rangle^{n+1} \qquad (2-27b)$$

where:

$$\left[\mathbf{A_x}\right] = \sum_{x-dir.\ elements}\left\{ \frac{\Delta y}{2}\frac{\overline{b\,D_{xx}}}{\Delta x}\begin{bmatrix}+1 & -1\\ -1 & +1\end{bmatrix} + \Delta y\,\bar{b}\,\frac{1}{\Delta t}\left[\mathbf{G}_{\mathbf{x}}^{'}\right]\right\}$$

$$\left[\mathbf{A_y}\right] = \sum_{y-dir.\ elements}\left\{ \frac{\Delta x}{2}\frac{\overline{b\,D_{yy}}}{\Delta y}\begin{bmatrix}+1 & -1\\ -1 & +1\end{bmatrix} + \Delta x\,\bar{b}\,\frac{1}{\Delta t}\left[\mathbf{G}_{\mathbf{y}}^{'}\right]\right\}$$

$$\left\langle \overset{*}{\mathbf{F}}_{\mathbf{yx}}\right\rangle^{n+1} = \sum_{x-dir.\ elements}\left\{ \frac{1}{4}\left\langle \begin{matrix}\Delta x\\ \Delta x\end{matrix}\right\rangle \left[ bD_{yx}\frac{\partial c^{*}}{\partial x}\bigg|_{y_2} - bD_{yx}\frac{\partial c^{*}}{\partial x}\bigg|_{y_1}\right]^{n+1}\right\}$$

$$\left\langle \hat{\mathbf{F}}_{\mathbf{x}}\right\rangle^{n} = \sum_{x-dir.\ elements}\Bigg\{ \Delta y\left[\mathbf{G}_{\mathbf{x}}^{'}\right]\Bigg( \frac{1}{2}\left\langle \frac{\partial}{\partial x}\left(\hat{b}\hat{D}_{xx}\frac{\partial \hat{c}}{\partial x}\right)\right\rangle^{n} + \frac{1}{2}\left\langle \frac{\partial}{\partial y}\left(\hat{b}\hat{D}_{yx}\frac{\partial \hat{c}}{\partial x}\right)\right\rangle^{n}$$

$$+ \left\langle \frac{\partial}{\partial y}\left(\hat{b}\hat{D}_{yy}\frac{\partial \hat{c}}{\partial y}\right)\right\rangle^{n} + \left\langle \frac{\partial}{\partial x}\left(\hat{b}\hat{D}_{xy}\frac{\partial \hat{c}}{\partial y}\right)\right\rangle^{n} + \left\langle \hat{b}\,\hat{c}\right\rangle^{n}\frac{1}{\Delta t}\Bigg)\Bigg\} = 0$$

$$\left\langle \mathbf{F_{xy}}\right\rangle^{n+1} = \sum_{y-dir.\ elements}\left\{ \frac{1}{4}\left\langle \begin{matrix}\Delta y\\ \Delta y\end{matrix}\right\rangle \left[ bD_{xy}\frac{\partial c}{\partial y}\bigg|_{x_2} - bD_{xy}\frac{\partial c}{\partial y}\bigg|_{x_1}\right]^{n+1}\right\}$$

$$\left\langle \hat{\mathbf{F}}_{\mathbf{y}}\right\rangle^{n} = \sum_{y-dir.\ elements}\left\{ \Delta x\left[\mathbf{G}_{\mathbf{y}}^{'}\right]\left( -\frac{1}{2}\left\langle \frac{\partial}{\partial y}\left(\hat{b}\hat{D}_{yy}\frac{\partial \hat{c}}{\partial y}\right)\right\rangle^{n} - \frac{1}{2}\left\langle \frac{\partial}{\partial x}\left(\hat{b}\hat{D}_{xy}\frac{\partial \hat{c}}{\partial y}\right)\right\rangle^{n}\right)\right\}$$

$$\left\{ \overset{*}{\mathbf{F}}\right\}^{n+1} = \sum_{y-dir.\ elements}\left\{ \Delta x\left[\mathbf{G}_{\mathbf{y}}^{'}\right]\left( \left\langle b\,c^{*}\right\rangle^{n+1}\frac{1}{\Delta t}\right)\right\}$$

The resulting systems of tri-diagonal matrix equations are solved using the FORTRAN routine *TRIDAG* presented in Carnahan, Luther, and Wilkes (1969).

## Solution of Additional Conservation of Mass Equations

The remaining terms in the aqueous phase PCB congener conservation of mass equation are represented as a third step in the numerical solution scheme by the following ordinary differential equation:

$$\frac{d\,c_{w_i}}{d\,t} = -\frac{\rho_b}{n}\,\alpha\left[k_{d_i}\,c_{w_i} - s_{2_i}\right] - \rho_o^*\,\alpha_{coll}\left[(k_d)_{coll_i}\,c_{w_i} - c_{o_i}\right] - \frac{\sigma_o}{n}\,\alpha_{coll}\left[(k_d)_{coll_i}\,c_{w_i} - S_{\sigma_i}\right] - \frac{I}{b\,n}\,(c_{w_i} - c_{w_{\inf_i}}) \qquad (2\text{-}28)$$

The remaining terms in the mobile colloidal phase PCB congener conservation of mass equation are:

$$\frac{d\,c_{o_i}}{d\,t} = \alpha_{coll}\left[(k_d)_{coll_i}\,c_{w_i} - c_{o_i}\right] - \lambda_o\,c_{o_i} - \frac{I}{b\,\rho_o^*\,n}\left[c_{o_i}\,\rho_o^* - (c_{o_i}\,\rho_o^*)_{\inf}\right] \qquad (2\text{-}29)$$

Similarly, the final terms in the mobile colloid conservation of mass equation are:

$$\frac{d\,\rho_o^*}{d\,t} = -\lambda_o\,\rho_o^* - \frac{I}{b\,n}\,(\rho_o^* - \rho_{o_{\inf}}^*) \qquad (2\text{-}30)$$

These three equations (Equations 2-10, 2-12, and 2-16) and the conservation of mass equations for immobile colloids (Equation 2-13), PCBs adsorbed to immobile colloids (Equation 2-15), and PCBs sorbed to soil (Equation 2-14) constitute a system of ordinary differential equations with respect to time. During each transport time step, $\Delta t$, the system of ODEs is solved implicitly using the fourth-order Runge-Kutta solver of Press et al. (1986). This solver employs adaptive step-size control in which the solver time step, $\delta t$, is automatically adjusted during the integration to maximize solution accuracy. For example, smaller time steps, $\delta t$, would be used for larger soil to pore water mass transfer rates.

## C.3.0 MODEL APPLICATION

### *C.3.1 Model Verification*

#### Test Problem 1—Analytical Solution for Equilibrium PCB Congener Transport

We first compare ***RATLIM2D_PCB*** simulation results with the analytical (exact mathematical) solution of Van Genuchten and Alves (1982) for one-dimensional solute transport in a porous medium with equilibrium partitioning between soil and groundwater. The groundwater does not contain colloids in this example. We used the principle of superposition (Bear 1979) to modify the analytical solution to handle the transport of multiple solutes in the form of a PCB congener mixture. We developed a FORTRAN code to compute the enhanced analytical solution. For this test problem, the distribution of PCB congeners is an Aroclor 1242 mixture from the literature (Frame et al., 1996). The congener $k_{oc}$ values are from Hansen et al. (1999).

Figure C-4 shows the longitudinal variations of total PCB concentration (i.e., sum of the congener concentrations) for the numerical (***RATLIM2D_PCB***) and analytical transport solutions at times of 20 and 50 years following the introduction of the upgradient source. Numerical results are shown for three values of the soil-water mass transfer coefficient, $\alpha$, in decreasing order of rate-limited sorption effects: $\alpha$ =0.365, 3.65, and 100,000 $yr^{-1}$ (0.001, 0.01, 270 $days^{-1}$). Table C-1 (Cosler 2004) summarizes several field and laboratory observations of $\alpha$ for a range of soil types. $\alpha$ =100,000 $yr^{-1}$ for the ***RATLIM2D_PCB*** simulation is equivalent to equilibrium soil-water partitioning and, as Figure C-4 illustrates, compares very well with the exact mathematical solution (solid black curve).

The congener simulation results on Figure C-4 illustrate an important characteristic of PCB transport—the more mobile, less-chlorinated homolog groups migrate much faster in the aquifer and create a "tail-like" zone of low level PCB concentrations in the leading edge of the plume. The numerical simulations for $\alpha$ =0.365 and 3.65 $yr^{-1}$ illustrate how rate-limited soil-water sorption further increases the degree of longitudinal dispersion (e.g., Culver et al., 1997; Cunningham et al., 1997).

#### Test Problem 2—*RATLIM2D_PCB* vs. *COLFRAC*

*COLFRAC* is a numerical model that simulates combined steady-state groundwater flow and transient, colloid-facilitated contaminant transport in porous or discretely fractured porous media (Ibaraki 2004). Computational efficiency for large-grid problems is achieved by employing a preconditioned, ORTHOMIN-accelerated iterative matrix solver. Groundwater flow and solute transport (including matrix diffusion and advection in the porous matrix) are rigorously treated in both fractures and porous matrix blocks. Chemical reactions in the form of first-order decay and linear equilibrium and kinetic sorption are also accommodated. The application of the program to complex real-world problems, which often require a fine spatial discretization, is facilitated by a pre-processor, PRECLD, which reads a data file containing relevant high-level descriptive information, and translates this information into a set of *COLFRAC* compatible input data files. Post-processing routines are then used to produce plotted or printed output.

We compared ***RATLIM2D_PCB*** simulation results with *COLFRAC* for a test problem involving one-dimensional solute (single constituent with a $k_{oc}$ similar to PCBs) transport in a porous medium with the following transport mechanisms—equilibrium partitioning between soil and groundwater; equilibrium partitioning between colloids and groundwater; and colloid filtration. Figure C-5 shows the simulated total (colloidal + aqueous phase) PCB, aqueous phase PCB, and mobile colloid concentrations for both codes. We show results with and without colloid filtration. The agreement between the codes is very good. Due to less accurate numerical methods, the *COLFRAC* results exhibit some numerical (artificial) dispersion in areas with large concentration gradients.

### Test Problem 3—RATLIM2D_PCB vs. RBCA Tier 2 Analyzer

The software package ***RBCA Tier 2 Analyzer*** (Cosler 2000) consists of two-dimensional groundwater flow and solute transport codes and an initial-condition plume generator that can easily be used to develop sophisticated and physically realistic models of groundwater systems and contaminant plumes. Five different transport simulation capabilities are provided: 1) single-constituent; 2) the PCE>TCE>DCE>VC sequential-decay sequence that occurs during the biodegradation of tetrachloroethene, trichloroethene, 1,2-dichloroethene, and vinyl chloride by reductive dechlorination; 3) instantaneous benzene-toluene-ethylbenzene-xylene (BTEX) biodegradation with a single electron acceptor (oxygen); 4) instantaneous BTEX biodegradation with multiple electron acceptors (oxygen, nitrate, iron(III), sulfate, carbon dioxide); and 5) kinetics-limited BTEX biodegradation with multiple electron acceptors.

The transport model has the capability of simulating either **equilibrium** or **non-equilibrium** (one-, two-, or multi-site sorption) partitioning between water and soil. The software can be used as a design tool for a wide variety of problems, including the analysis of remedial alternatives such as groundwater pump and treat systems (including extraction well concentration “tailing” effects), natural attenuation evaluation, and source remediation level determination based on simulation of compliance point concentrations. ***RBCA Tier 2 Analyzer*** features a Windows-based visual graphical environment for grid construction, data input, initial-condition plume generation, and automated and user-defined boundary condition specification; optional import of contoured contaminant plumes saved in the **Surfer** GRD format; detailed help system with numerous fate and transport parameter values from the literature; low computer memory requirements; fast execution times; and sophisticated visualization and analysis of simulation results using the graphics program **Tecplot** developed by Amtec Engineering.

In this test, we compare ***RATLIM2D_PCB*** and ***RBCA Tier 2 Analyzer*** for the Test Problem 2 parameters but remove the colloids. However, we add rate-limited soil to groundwater partitioning as a transport mechanism. Figure C-6 shows the excellent agreement between simulation results for both models and three values of the soil-water mass transfer coefficient $\alpha$: 1, 10, and 1,000 day$^{-1}$. $\alpha$ =1,000 day$^{-1}$ represents approximate equilibrium soil to water partitioning. As discussed above and illustrated on Figure C-6, non-equilibrium soil to groundwater partitioning (i.e., low values of $\alpha$ ) is similar to increased longitudinal dispersion (also, see Haggerty and Gorelick 1995 and 1998).

## C.3.2 Model Input Data

### Hydrogeologic and PCB Fate and Transport Data

From the model calibration process and site-specific measurements, we estimated the following parameter values for the final model simulation results presented in the RI report:

#### Soil to Water Mass Transfer Rate, $\alpha$

Table C-1 shows representative values for other sites. Based on model calibration: $\alpha$ = 0.1 yr$^{-1}$

#### Longitudinal Dispersivity, $a_L$

Table C-2 lists measurements from other sites. Based on model calibration: $a_L$ = 1 m

### *Groundwater Pore Velocity, u*

We used a uniform velocity field equivalent to the approximate mean groundwater pore velocity along the PCB plume centerline. Based on site hydraulic conductivity and hydraulic gradient measurements: $u \approx$ 3,670 m/yr.

### *Fraction of Organic Carbon in Soil, $f_{oc}$*

From site measurements, $f_{oc} \approx 0.001$. Table C-3 summarizes $f_{oc}$ measurements from other sites. As outlined in Table C-4, we used $f_{oc}$ and the organic carbon/ water partition coefficient, $k_{oc}$, to estimate site-specific soil-water partition coefficients, $k_d$, for each PCB congener.

### *Organic Carbon/Water Partition Coefficient, $k_{oc}$*

We used the compound-specific PCB congener $k_{oc}$ values estimated by Hansen et al. (1999) as initial estimates. We made some adjustments of these values (within appropriate uncertainty ranges) during model calibration.

### *Colloid – Water Mass Transfer Coefficient, $\alpha_{coll}$*

From model calibration: $\alpha_{coll} \approx$ 100 yr$^{-1}$.

### *Fraction of Organic Carbon in Colloid, $(f_{oc})_{coll}$*

From model calibration: $(f_{oc})_{coll} \approx 0.054$. Site-specific colloid characterization studies (Hart Crowser 2005) indicate that the colloids are primarily quartz minerals with particle sizes ranging from <0.3 to >25 $\mu$m. The effective diameter of the majority of particles was <1.6 $\mu$m. As shown in Table C-5, the colloidal size range in groundwater is about 0.01 to 10 $\mu$m, with the smallest colloids being those that are just larger than dissolved macromolecules, and the largest colloids being those that resist settling once suspended in soil pore waters (DeNovio et al., 2004).

Because the colloids at the site are predominantly inorganic, $(f_{oc})_{coll}$ was a calibration parameter used to estimate the colloid-water partition coefficient, $(k_d)_{coll}$, which quantifies chemical sorption to inorganic soil/particles (e.g., Lyman, et al., 1982).

### *Colloid Filtration Coefficient,* $f_c$

From model calibration: $f_c \approx 0.002$ m$^{-1}$. As a comparison, Ibaraki and Sudicky (1995) characterize $f_c \ll 0.1$ m$^{-1}$ as "weak" filtration and $f_c \gg 10$ m$^{-1}$ as "vigorous" filtration.

### Boundary and Initial Conditions

The PCB congener and colloid transport model incorporates fixed concentration boundary conditions along the upgradient boundary of the simulation domain that are based on monitoring well data. In effect, these boundary conditions simulate a source of PCB contamination in the general vicinity of monitoring well RM-MW-17S. We set all initial ($t = 0$) concentrations to zero because the model simulations were designed to mimic the historical evolution of the PCB plume.

DeNovio et al. (2004) report several field studies of colloid transport in groundwater systems where the colloid concentrations generally exceeded 1 to 10 mg/L. Ryan and Elimelech (1996) report groundwater colloid concentrations as high as 100 mg/L in samples taken from a wide variety of geological and geochemical settings. Total suspended solids (TSS) concentration measurements for monitoring well RM-MW-17S have generally ranged from 5 to 45 mg/L. Observed TSS concentrations in upgradient monitoring wells include: RM-MW-15S (2 to 67 mg/L); RM-MW-16S (3 to 21 mg/L); RM-MW-1S (2 to 34 mg/L); and HL-MW-29S (2 to 13 mg/L). Based on this information, we assumed 10 mg/L as the upgradient colloid concentration boundary condition. However, the simulation results are not very sensitive to this value because the colloid-water partition coefficient, $(k_d)_{coll}$, was determined by model calibration, as discussed above. In other words, the product of the colloid concentration and $(k_d)_{coll}$ determines the significance of colloid transport on the downgradient PCB congener distribution in groundwater.

## C.4.0 REFERENCES FOR APPENDIX C

Baes, C.F., and R.D. Sharp 1983. A proposal for estimation of soil leaching and leaching constants for use in assessment models. *Journal of Environmental Quality* 12, 17-28.

Bahr, J.M., and J. Rubin 1987. Direct comparison of kinetic and local equilibrium formulations for solute transport affected by surface reactions. *Water Resources Research* 23, 438-452.

Ball, W.P., and P.V. Roberts 1991. Long-term sorption of halogenated organic chemicals by aquifer material. 2. Intraparticle diffusion. *Environmental Science & Technology* 25, 1237-1249.

Baptista, A.M., 1987. Solution of advection-dominated transport by eulerian-lagrangian methods using the backwards method of characteristics. Ph.D. diss., Massachusetts Institute of Technology, Cambridge, Massachusetts.

Barbee, G.C., 1994. Fate of chlorinated aliphatic hydrocarbons in the vadose zone and ground water. *Ground Water Monitoring & Remediation* 14(1), 129-140.

Barrio-Lage, G.A., F.Z. Parsons, R.S. Nassar, and P.A. Lorenzo 1987. Biotransformation of trichloroethene in a variety of subsurface materials. *Environ. Toxicol. Chem*. 6, 571-578.

Barrio-Lage, G.A., F.Z. Parsons, R.M. Narbaitz, and P.A. Lorenzo 1990. Enhanced anaerobic biodegradation of vinyl chloride in ground water. *Environ. Toxicol. Chem*. 9, 403-415.

Bear, J., 1972. *Dynamics of Fluids in Porous Media*. New York: Dover Publications, Inc.

Bear, J., 1979. *Hydraulics of Groundwater*. New York: McGraw-Hill.

Benker, E., G.B. Davis, S. Appleyard, D.A. Berry, and T.R. Power 1994. Groundwater contamination by trichloroethene (TCE) in a residential area of Perth: Distribution, mobility, and implications for management. In *Proceedings - Water Down Under '94,* 25th Congress of IAH, Adelaide, South Australia, November 1994.

Bentley, L.R., and G.F. Pinder 1992. Eulerian-lagrangian solution of the vertically averaged groundwater transport equation. *Water Resources Research* 28, 3011-3020.

Borden, R.C., and P.B. Bedient 1986. Transport of dissolved hydrocarbons influenced by oxygen limited biodegradation – theoretical development. *Water Resources Research* 22, 1973-1982.

Bouwer, E.J., and P.L. McCarty 1983. Transformations of 1- and 2-carbon halogenated aliphatic organic compounds under methanogenic conditions. *Appl. Environ. Microbiol*. 45, 1286-1294.

Brusseau, M.L., T. Larsen, and T.H. Christensen 1991. Rate-limited sorption and nonequilibrium transport of organic chemicals in low organic carbon aquifer materials. *Water Resources Research* 27, 1137-1145.

Carnahan, B., H.A. Luther, and J.O. Wilkes 1969. *Applied Numerical Methods*. New York: John Wiley & Sons, Inc.

Carroll, K.M., M.R. Harkness, A.A. Bracco, and R.R. Balcarcel 1994. Application of a permeant/polymer diffusional model to the desorption of polychlorinated biphenyls from Hudson River sediments. *Environmental Science & Technology* 28, 253-258.

Carslaw, H.S., and J.C. Jaeger 1959. *Conduction of Heat in Solids*. Oxford: Clarendon Press.

Chapelle, F.H., 1994. Assessing the efficiency of intrinsic bioremediation. EPA/540/R-94/515. Washington, D.C.: U.S. Environmental Protection Agency.

Connaughton, D.F., J.R. Stedinger, L.W. Lion, and M.L. Shuler 1993. Description of time-varying desorption kinetics: release of napthalene from contaminated soils, *Environmental Science & Technology* 27, 2397-2403.

Cornelissen, G., P.C.M. van Noort, J.R. Parsons, and H.A.J. Govers 1997. Temperature dependence of slow adsorption and desorption kinetics of organic compounds in sediments. *Environmental Science & Technology* 31, 454-460.

Cosler, D.J., 2000. Risk-Based Correction Action (RBCA) Tier 2 Analyzer, Two-Dimensional Groundwater Flow and Biodegradation Model, Ref. Manual. Waterloo Hydrogeologic, Inc., Waterloo, Ontario, Canada.

Cosler, D.J., 2004. Effects of Rate-Limited Mass Transfer on Water Sampling with Partially Penetrating Wells. *Ground Water* 42, no. 2: 203-222.

Cox, E., E. Edwards, L. Lehmicke, and D. Major 1995. Intrinsic biodegradation of trichloroethylene and trichloroethane in a sequential anaerobic-aerobic aquifer. In *Intrinsic Bioremediation*, eds. R.E. Hinchee, J.T. Wilson, and D.C. Downey, Battelle Press, Columbus, OH, 223-231.

Culver, T.B., S.P. Hallisey, D. Sahoo, J.J. Deitsch, and J.A. Smith 1997. Modeling the desorption of organic contaminants from long-term contaminated soil using distributed mass transfer rates. *Environmental Science & Technology* 31, 1581-1588.

Cunningham, J.A., C.J. Werth, M. Reinhard, and P.V. Roberts 1997. Effects of grain-scale mass transfer on the transport of volatile organics through sediments 1. Model development. *Water Resources Research* 33, 2713-2726.

Cushey, M.A., and Y. Rubin 1997. Field-scale transport of nonpolar organic solutes in 3-D heterogeneous aquifers. *Environmental Science & Technology* 31, 1259-1268.

Davis, J.W., and C.L. Carpenter 1990. Aerobic biodegradation of vinyl chloride in ground-water samples. *Appl. Environ. Microbiol*. 56, 3878.

Daus, A.D., and E.O. Frind 1985. An alternating direction Galerkin technique for simulation of contaminant transport in complex groundwater systems. *Water Resources Research* 21, 653-664.

DeNovio, N.M., J.E. Saiers, and J.N. Ryan 2004. Colloid Movement in Unsaturated Porous Media. *Vadose Zone Journal* 3: 338-351.

Domenico, P.A., and F.W. Schwartz 1990. *Physical and Chemical Hydrogeology*. New York: John Wiley & Sons.

Douglas, J., Jr. Alternating direction methods for three space variables. *Numer. Math*. 4, 41.

Dupont, R.R., K. Gorder, D.L. Sorenson, M.W. Kemblowski, and P. Haas 1996. Case Study: Eielson Air Force Base, Alaska. In *Proceedings of the Symposium on Natural Attenuation of Chlorinated Organics in Ground Water, Dallas, TX*: EPA/540/R-96/509, September 1996.

Ehlke, T.A., B.H. Wilson, J.T. Wilson, and T.E. Imbrigiotta 1994. In-situ biotransformation of trichlorethylene and cis-1,2-dichloroethylene at Picatinny Arsenal, New Jersey. In *Proceedings of the U.S. Geological Survey Toxic Substances Hydrology Program*, eds. D.W. Morganwalp and D.A. Aranson, Water Resources Investigation Report 94-4014.

Ellis, D.E., E.J. Lutz, G.M. Klecka, D.L. Pardieck, J.J. Salvo., M.A Heitkamp, D.J. Gannon, C.C. Mikula, C.M. Vogel, G.D. Sayles, D.H. Kampbell, J.T. Wilson, and D.T. Maiers 1996. Remediation technology development forum intrinsic remediation project at Dover Air Force Base, Delaware. In *Proceedings of the Symposium on Natural Attenuation of Chlorinated Organics in Ground Water, Dallas, TX*: EPA/540/R-96/509, September 1996.

EPA 1989. Evaluation of ground-water extraction remedies, volume 1, summary report. U.S. Environmental Protection Agency, Office of Emergency and Remedial Response. Report EPA/540/2-89/054.

Evans, M., N. Hastings, and B. Peacock 1993. *Statistical Distributions*, 2nd ed. New York: John Wiley & Sons, Inc.

Feehley, C.E., C. Zheng, and F.J. Molz 2000. A dual-domain mass transfer approach for modeling solute transport in heterogeneous aquifers: application ot the macrodispersion experiment (MADE) site. *Water Resources Research* 36, 2501-2515.

Fetter, C.W., 1993. *Contaminant Hydrogeology*. New York: Macmillan.

Fogel, M.M., A.R. Taddeo, and S. Fogel 1986. Biodegradation of chlorinated ethenes by a methane-utilizing mixed culture. *Applied and Environmental Microbiology* 51(4), 720-724.

Frame, G.M., J.W. Cochran, and S.S. Boewadt 1996. *Journal of High Resolution Chromatography* 19, 657-668.

Gelhar, L.W., C. Welty, and K.R. Rehfeldt 1992. A critical review of data on field-scale dispersion in aquifers. *Water Resources Research* 28, 1955-1974.

Gelhar, L.W., 1993. *Stochastic Subsurface Hydrology*. Prentice Hall.

Gorder, K.A., R.R. Dupont, D.L. Sorenson, M.W. Kemblowski, and J.E. McLean 1996. Analysis of intrinsic bioremediation of trichloroethene-contaminated ground water at Eielson Air Force Base, Alaska. In *Proceedings of the Symposium on Natural Attenuation of Chlorinated Organics in Ground Water, Dallas, TX, September 11-13, 1996*: EPA/540/R-96/509.

Haggerty, R., and S.M. Gorelick 1995. Multiple-rate mass transfer for modeling diffusion and surface reactions in media with pore-scale heterogeneity. *Water Resources Research* 31, 2383-2400.

Haggerty, R., and S.M. Gorelick 1998. Modeling mass transfer processes in soil columns with pore-scale heterogeneity. *Soil Science Society of America Journal* 62, 62-74.

Hansch, C., and A.J. Leo 1979. *Substituent Constants for Correlation Analysis in Chemistry and Biology*. New York: John Wiley & Sons, Inc.

Hansen, B.G., A.B. Paya-Perez, M. Rahman, and B.R. Larsen 1999. QSARs for $K_{ow}$ and $K_{oc}$ of PCB Congeners: A Critical Examination of Data Assumptions and Statistical Approaches. *Chemosphere* 39(13), 2209-2228.

Harmon, T.C., and P.V. Roberts 1994. The effect of equilibration time on desorption rate measurements with chlorinated alkenes and aquifer particles. *Environmental Progress* 13(1), 1-8.

Harmon, T.C., L. Semprini, and P.V. Roberts 1992. Simulating solute transport using laboratory-based sorption parameters. *Journal of Environmental Engineering*, Am. Soc. Civ. Eng. 118, 666-689.

Hart Crowser 2005. Laboratory-Scale Treatability Study, Phase II and III Batch Tests and Particle Characterization, Casting Groundwater PCB Plume, Kaiser Trentwood Facility. Prepared for Kaiser Aluminum & Chemical Corp., May 2, 2005, Project Report 2644-82/86.

Harvey, C., and S.M. Gorelick 2000. Rate-limited mass transfer or macrodispersion: Which dominates plume evolution at the Macrodispersion Experiment (MADE) site?. *Water Resources Research* 36, 637-650.

Haston, Z.C., P.K. Sharma, J.N.P. Black, and P.L. McCarty 1994. Enhanced reductive dechlorination of chlorinated ethenes. In *Proceedings of the EPA Symposium on Bioremediation of Hazardous Wastes: Research, Development, and Field Evaluations*, EPA/600/R-94/075.

Healy, R.W., and T.F. Russell 1989. Efficient implementation of the modified method of characteristics in finite-difference models of solute transport. In *Solving Ground Water Problems with Models*, Proceedings of the Fourth International Conference on the Use of Models to Analyze and Find Working Solutions to Ground Water Problems. Indianapolis, IN: NWWA and IGWMC.

Henson, J.M., M.V. Yates, and J.W. Cochran 1989. Metabolism of chlorinated methanes, ethanes, ethylenes by a mixed bacterial culture growing off methane. *J. Ind. Microbiol.* 4, 29-35.

Huebner, K.H., 1975. *The Finite Element Method for Engineers*. New York: John Wiley & Sons, Inc.

Ibaraki, M., 2004. COLFRAC User's Guide, A Numerical Model for Two-Dimensional, Saturated Groundwater Flow and Colloid-Facilitated Solute Transport in Porous or Discretely-Fractured Porous Media. Department of Geological Sciences, The Ohio State University, Columbus, Ohio.

Ibaraki, M., and E.A. Sudicky 1995. Colloid-Facilitated Contaminant Transport in Discretely Fractured Porous Media 1. Numerical Formulation and Sensitivity Analysis. *Water Resources Research* 31(12), 2945-2960.

Karickhoff, S.W., 1981. Semi-empirical estimation of sorption of hydrophobic pollutants on natural sediments and soils. *Chemosphere* 10, 833-846.

Keely, J.F., 1989. Performance evaluations of pump-and-treat remediations. U.S. Environmental Protection Agency, Office of Research and Development. Report EPA/540/4-89/005.

Klecka, G.M., S.J. Gonsior, and D.A. Markham 1990. Biological transformations of 1,1,1-trichloroethane in subsurface soils and ground water. *Environ. Toxicol. Chem*. 9, 1437-1451.

Koyama, T., 1964. Gaseous metabolism in lake sediments and paddy soils. In *Advances in Organic Geochemistry*, eds. U. Colombo and G.D. Hobson. New York: Macmillan Co. 363-375.

Lapidus, L., and G.F. Pinder 1982. Numerical Solution of Partial Differential Equations in Science and Engineering. New York: John Wiley & Sons, Inc.

Lyman, W.J., W.F. Reehl, and D.H. Rosenblatt 1982. *Handbook of Chemical Property Estimation Methods*. New York: McGraw-Hill.

Lee, M.D., P.F. Mazierski, R.J. Buchanan, D.E. Ellis, and L.S. Sehayek 1995. Intrinsic and in situ anaerobic biodegradation of chlorinated solvents at an industrial landfill. In *Intrinsic Bioremediation*, eds. R.E. Hinchee, J.T. Wilson, and D.C. Downey, 205-222, Columbus, Ohio: Battelle Press.

Lu, G., T.P. Clement, C. Zheng, and T.H. Wiedemeier. Natural attenuation of BTEX compounds: model development and field-scale application. *Ground Water* 37, 707-717.

Lyman, W.J., W.F. Reehl, and D.H. Rosenblatt 1982. *Handbook of Chemical Property Estimation Methods*. McGraw-Hill.

MacIntyre, W.G., M. Boggs, C.P. Antworth, and T.B. Stauffer 1993. Degradation kinetics of aromatic organic solutes introduced into a heterogeneous aquifer. *Water Resources Research* 29, 4045-4051.

Mackay, D.M., and J.A. Cherry 1989. Groundwater contamination: pump and treat remediation. *Environmental Science & Technology* 23, 630-636.

Mackay, D.M., 1990. Characterization of the distribution and behavior of contaminants in the subsurface. In *Ground Water and Soil Contamination Remediation: Toward Compatible Science, Policy, and Public Perception*. Washington, D.C.: National Academy Press, 70-90.

Mortimer, C.H., 1981. The oxygen content of air-saturated fresh waters over ranges of temperature and atmospheric pressure of limnological interest. *Mitt. Int. Ver. Limnol* 22.

National Academy Press 1994. Alternatives for ground water cleanup. Washington, D.C.

Nyer, E.K., 2000. Treatment Technology: Looking forward. *Ground Water Monitoring & Remediation* 20(1), 48-51.

Parsons, F., P.R. Wood, and J. DeMarco 1984. Transformations of tetrachloroethene and trichloroethene in microcosms and groundwater. *Journal American Water Works Association* 76, 56-59.

Pedit, J.A., and C.T. Miller 1994. Heterogeneous sorption processes in subsurface systems. 1. Model formulations and applications. *Environmental Science & Technology* 28, 2094-2104.

Pedit, J.A., and C.T. Miller 1995. Heterogeneous sorption processes in subsurface systems. 2. Diffusion modeling approaches. *Environmental Science & Technology* 29, 1766-1772.

Pickens, J.F., and G.E. Grisak 1981. Scale-dependent dispersion in a stratified granular aquifer. *Water Resources Research* 17, 1191-1211.

Pollock, D.W., 1988. Semianalytical computation of path lines for finite-difference models. *Ground Water* 26, 743-750.

Press, W.H., B.P. Flannery, S.A. Teukolsky, and W.T. Vetterling 1986. *Numerical Recipes*. Cambridge University Press.

Rifai, H., R. Borden, J. Wilson, and C. Ward 1995. Intrinsic bioattenuation for subsurface restoration. In *Intrinsic Bioremediation*, eds. R.E. Hinchee, J.T. Wilson, and D.C. Downey, 1-30, Columbus, Ohio: Battelle Press.

Saunders, F.Y., and V. Maltby 1996. Degradation of chloroform under anaerobic soil conditions. In Proceedings of the Symposium on Natural Attenuation of

Chlorinated Organics in Ground Water, Dallas, TX, September 11-13, 1996: EPA/540/R-96/509.

Seth, R., D. Mackay, and J. Muncke 1999. Estimating the organic carbon partition coefficient and its variability for hydrophobic chemicals. *Environmental Science & Technology* 33, 2390-2394.

Smith, J.A., D. Sahoo, H.M. McLellan, and T.E. Imbrigiotta 1997. Surfactant-enhanced remediation of a trichloroethene-contaminated aquifer. 1. Transport of triton X-100. *Environmental Science & Technology* 31, 3565-3572.

Stauffer, T.B., T.B Antworth, J.M. Boggs, and W.G. MacIntyre 1994. A natural gradient tracer experiment in a heterogeneous aquifer with measured in situ biodegradation rates: a case for natural attenuation. In *Symposium on Natural Attenuation of Ground Water*, EPA/600/R-94/162, 68-74. Washington, D.C.: U.S. Environmental Protection Agency.

Swanson, M., T.H. Wiedemeier, D.E. Moutoux, D.H. Kampbell, and J.E., Hansen 1996. Patterns of natural attenuation of chlorinated aliphatic hydrocarbons at Cape Canaveral Air Station, Florida. In *Proceedings of the Symposium on Natural Attenuation of Chlorinated Organics in Ground Water, Dallas, TX, September 11-13, 1996*: EPA/540/R-96/509.

Van Genuchten, M.Th., and W.J. Alves 1982. *Analytical Solutions of the One-Dimensional Convective-Dispersive Solute Transport Equation*. U.S. Department of Agriculture, Technical Bulletin No. 1661, 151 pp.

Van Genuchten, M.Th., and R.J. Wagenet 1989. Two-site/two-region models for pesticide transport and degradation: theoretical development and analytical solutions. *Soil Science Society of America Journal* 53, 1303-1310.

Vogel, T.M., and P.L. McCarty 1987. Abiotic and biotic transformations of 1,1,1-trichloroethane under methanogenic conditions. *Environmental Science & Technology* 21, 1208-1213.

Walton, W.C., 1988. *Practical Aspects of Groundwater Modeling*. Worthington, OH: National Water Well Association.

Weaver, J.W., J.T. Wilson, and D.H. Kampbell 1996. Extraction of degradation rate constants from the St. Joseph, Michigan, trichloroethene site. In *Proceedings of the Symposium on Natural Attenuation of Chlorinated Organics in Ground Water, Dallas, TX, September 11-13, 1996*: EPA/540/R-96/509.

Werth, C.J., J.A. Cunningham, P.V. Roberts , and M. Reinhard 1997. Effects of grain-scale mass transfer on the transport of volatile organics through sediments 2. Column results. *Water Resources Research* 33, 2727-2740.

Werth, C.J., and M. Reinhard 1997. Effects of temperature on trichloroethylene desorption from silica gel and natural sediments. 2. Kinetics. *Environmental Science & Technology* 31, 697-703.

Wetzel, R.G., 1972. The role of carbon in hard-water marl lakes. In *Nutrients and Eutrophication: The Limiting-Nutrient Controversy*, ed. G.E. Likens, Special Symposium, Amer. Soc. Limnol. Oceanogr. 1, 84-97.

Wetzel, R.G., 1983. *Limnology*, 2nd ed. Orlando: Saunders College Publishing.

Wiedemeier, T.H., J.T. Wilson, and R.N. Miller 1995. Significance of anaerobic processes for the intrinsic bioremediation of fuel hydrocarbons. In *Proceedings of the Petroleum Hydrocarbons and Organic Chemicals in Ground Water: Prevention, Detection, and Restoration Conference*, NWWA/API.

Wiedemeier, T.H., J.T. Wilson, D.H. Kampbell, R.N. Miller, and J.E. Hansen 1995b. Technical protocol for implementing intrinsic remediation with long-term monitoring for natural attenuation of fuel contamination dissolved in groundwater. San Antonio, TX: U.S. Air Force Center for Environmental Excellence.

Wiedemeier, T.H., M.A. Swanson, J.T. Wilson, D.H. Kampbell, R.N. Miller, and J.E. Hansen 1996. Approximation of biodegradation rate constants for monoaromatic hydrocarbons (BTEX) in ground water. *Ground Water Monitoring & Remediation* 16(3), 186-194.

Wiedemeier, T.H., J.T. Wilson, and D.H. Kampbell 1996c. Natural attenuation of chlorinated aliphatic hydrocarbons at Plattsburgh Air Force Base, New York. In *Proceedings of the Symposium on Natural Attenuation of Chlorinated Organics in Ground Water, Dallas, TX, September 11-13, 1996*: EPA/540/R-96/509.

Wilson, B.H., J.T. Wilson, D.H. Kampbell, B.E. Bledsoe, and J.M. Armstrong 1990. Biotransformation of monoaromatic and chlorinated hydrocarbons at an aviation gasoline spill site. *Geomicrobiology Journal* 8, 225-240.

Wilson, B.H., T.A. Ehlke, T.E. Imbrigiotta, and J.T. Wilson 1991. Reductive dechlorination of trichlorethylene in anoxic aquifer material from Picatinny Arsenal, New Jersey. In *Proceedings of the U.S. Geological Survey Toxic*

*Substances Hydrology Program*, eds. G.E. Mallard and D.A. Aranson, Water Resources Investigation Report 91-4034, 704-707.

Wilson, B.H., J.T. Wilson, and D. Luce 1996. Design and interpretation of microcosm studies for chlorinated compounds. In *Proceedings of the Symposium on Natural Attenuation of Chlorinated Organics in Ground Water, Dallas, TX, September 11-13, 1996*: EPA/540/R-96/509.

Wilson, J.T., J.F. McNabb, B.H. Wilson, and M.J. Noonan 1982. Biotransformation of selected organic pollutants in groundwater. *Developments in Industrial Microbiology* 24, 225-233.

Wilson, J.T., J.F. McNabb, D.L. Balkwill, and W.C. Ghiorse 1983. Enumeration and characteristics of bacteria indigenous to a shallow water-table aquifer. *Ground Water* 21, 134-142.

Wilson, J.T., F.M. Pfeffer, J.W. Weaver, D.H. Kampbell, T.H. Wiedemeier, J.E. Hansen, and R.N. Miller 1994. Intrinsic bioremediation of JP-4 jet fuel. EPA/540/R-94/515. Washington, D.C.: U.S. Environmental Protection Agency.

Wilson, J.T., L.E. Leach, M. Henson, and J.N. Jones 1986. In situ biorestoration as a groundwater remediation technique. *Ground Water Monitoring Review*, Fall 1986, 56-64.

Xu, M., and Y. Eckstein 1995. Use of weighted least-squares method in evaluation of the relationship between dispersivity and scale. *Ground Water* 33, 905-908.

Zhang, W., E.J. Bouwer, and W.P. Ball 1998. Bioavailability of hydrophobic organic contaminants: effects and implications of sorption-related mass transfer on bioremediation. *Ground Water Monitoring & Remediation* 18(1), 126-138.

L:\Jobs\2644114\GW RI\Final Appendix C.doc

**Table C-1 - One- and Two-Site Models**
**Mass Transfer Rate, $\alpha$, and Fraction of Soil Mass at Equilibrium, F**

| Source of Estimate | $\alpha$ in days$^{-1}$ | F | Material: Description | Material: $f_{oc}$ | Reference |
|---|---|---|---|---|---|
| Batch sorption studies (30 days) with TCE, vinyl chloride, carbon tetrachloride | 0.02 to 0.15 | NA | sand and gravel | 0.0011 | Moffett Naval Air Station, California (Harmon et al., 1992) |
| Laboratory measurement of napthalene desorption rates using fresh (days to weeks) and aged (30 years) soil samples | 16 (3 days)<br>0.36 (3 months)<br>0.15 (aged)<br>6.7 to 14 (aged)<br>13 (aged)<br>5.2 (aged) | NA<br>0.74<br>0.36<br>NA<br>NA<br>NA | - | 0.0036<br>0.0036<br>0.13<br>0.016<br>0.0023<br>0.012 | Manufactured gas plant site, northeastern U. S. (Connaughton et al., 1993) |
| Batch sorption studies (150 days) with PCE[a] | 0.24<br>0.15 | NA<br>0.10 | fine to coarse sand | 0.00021 | Borden, Ontario (Ball and Roberts 1991) |
| Column desorption studies (21 days) with TCE[a] | 0.17<br>0.014 | NA<br>NA | medium sand<br>fine sand | 0.0015<br>0.00064 | Aquifer sediment (Werth and Reinhard 1997) |
| Laboratory batch (20 days), column (42 days), and field injection (23 days) experiments with Triton X-100 (non-ionic surfactant) | 0.27 (lab)<br>0.13 (column)<br>0.013 (field) | 0.47<br>0.19<br>0.15 | sand and gravel | 0.0008 | Picatinny Arsenal, New Jersey (Smith et al., 1997) |
| Field-scale natural gradient experiment with PCE (700 days) | 0.0046 | 0.32 | medium to fine sand | 0.00021 | Borden, Ontario (Cushey and Rubin 1997) |
| Laboratory column studies with several hydrophobic organic chemicals and three low-organic carbon aquifer materials | 0.48 to 2.4 | 0.42 to 0.61 | sand | 0.00007 to 0.00025 | Brusseau et al., 1991 |
| Laboratory studies of desorption of chlorobenzenes, PCBs, and PAHs from lab- and field-contaminated sediments (13 to 90 days) — Lab | 0.024 to 0.098 (slow)<br>0.007 to 0.012 (very slow) | 0.34 to 0.91 | very fine sand | 0.032 | Lake sediments, The Netherlands (Cornelissen et al., 1997) |
| Field | 0.02 to 0.05 (slow)<br>0.003 to 0.006 (very slow) | 0.1 to 0.4 | fine sand and silt | 0.070 | |
| Long-term (12 months) laboratory desorption experiments with PCB-contaminated river sediments[a] | 0.00055<br>0.00083 | 0.55<br>0.76 | very fine to coarse sand, some silt | 0.010<br>0.046 | Hudson Rivers sediments (Carroll et al., 1994) |
| Laboratory batch sorption experiments (160 days) with diuron (herbicide) | 0.026<br>0.0067 | NA<br>0.098 | fine to very coarse sand | 0.00043 | Subsurface material (Wagner) from sand and gravel pit (Pedit and Miller 1994 and 1995) |
| Laboratory batch sorption experiments (8 to 10 days) with PCE and TCE (Harmon and Roberts 1994) | 0.11 to 0.19 | NA | medium to fine sand | 0.0002 | Borden, Ontario |
| | 0.032 to 0.36 | NA | coarse sand | 0.001 | Moffett Naval Air Station, California |
| Field-scale natural gradient experiment with bromide and tritium (500 days) | 0.0046 (bromide)<br>0.011 (tritium) | NA | sand and gravel, small amounts silt/clay | - | Columbus Air Force Base, Mississippi (Harvey and Gorelick 2000) |
| | 0.0016 to 0.0033 (tritium) | | | | Feehley et al., 2000 |

Tables from Cosler (2004)
NA=not analyzed because data were fit to a one-site model
[a]First-order mass transfer rate converted from spherical diffusion value using first term of the first-order, multi-rate series approximation to the diffusion model (Haggerty and Gorelick 1995)

L:\Jobs\2644114\GW RI\Appendix C\PCB_Model_Appendix C_Tables.doc

**Table C-2 - Dispersion Coefficients and Dispersivity**

Longitudinal Dispersivity, $a_L$

Use the graph below or the following line-of-best-fit equation to estimate the longitudinal dispersivity at your site:

$$a_L = 0.83\left[\log_{10}(L_S)\right]^{2.414} \quad \text{(Xu and Eckstein 1995)}$$

where $L_S$ is the horizontal length scale of the plume and $a_L$ and $L_S$ are in meters.

Transverse Dispersivity, $a_T$

The ratio of transverse ($a_T$) to longitudinal dispersivity, $a_T/a_L$, is typically in the range of 0.05 to 0.25 (Fetter 1993).

Molecular Diffusion Coefficient

The molecular diffusion coefficient for a porous medium, $\tilde{D}_m$, is defined as:

$$\tilde{D}_m = \tau D_m$$

where $\tau$ is the tortuosity of the aquifer and $D_m$ is the molecular diffusion coefficient of the solute in free water. Bear (1972) cites references indicating $0.3 \le \tau \le 0.7$ as a representative range for unconsolidated media. At normal groundwater temperatures, most chemicals exhibit a molecular diffusion coefficient in water, $D_m$, of about $1\times10^{-9}$ $m^2/s$ (Lyman et al., 1982).

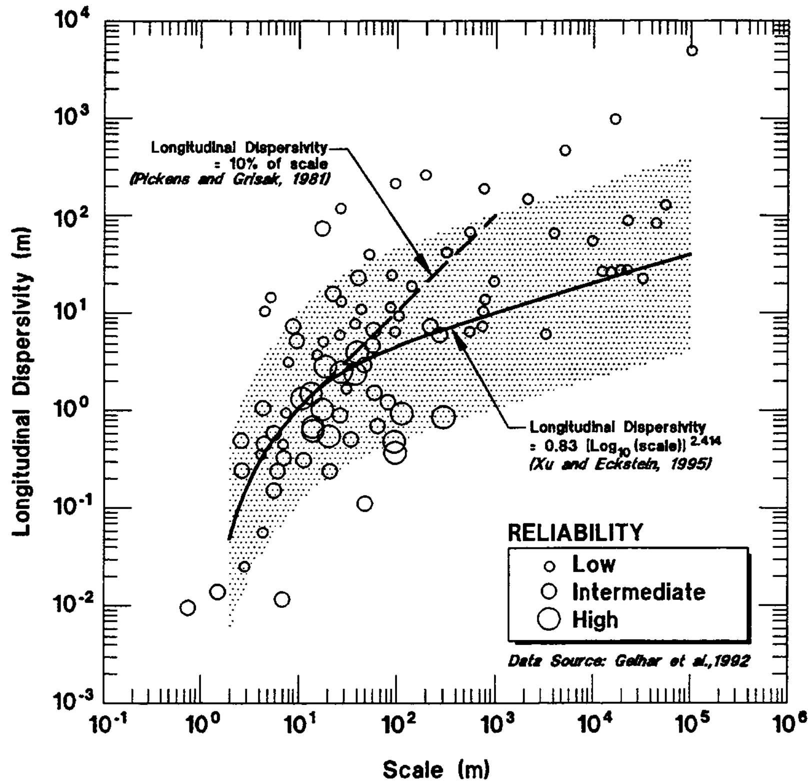

## Table C-3 - Organic Carbon Content ($f_{oc}$) of Typical Sand and Gravel Aquifers

| Site Location | Organic Carbon Content, $f_{oc}$ | Material |
|---|---|---|
| Gloucester, Ontario | 0.001 to 0.006 | interstratified silts, sands, gravels |
| Borden, Ontario | 0.0002 | medium to fine sand |
| Moffett Naval Air Station, California | 0.0011 | sand and gravel |
| Otis Air Force Base, Massachusetts | 0.0001 to 0.0075 | sand and gravel |
| Savage Well Superfund Site, New Hampshire | 0.0014 to 0.0030 | fine to coarse sand and gravel |
| Gallup's Quarry Superfund Site, Connecticut | 0.001 to 0.002 | fine to coarse sand and gravel |
| Old Southington Landfill Superfund Site, Connecticut | 0.0005 to 0.003 | sand and gravel |
| Darling Hill Superfund Site, Vermont | 0.0014 to 0.0039 | fine to coarse sand |
| Parker Landfill Superfund Site, Vermont | 0.0003 to 0.011 | very fine to medium sand |
| Hill Airforce Base, Utah | 0.00053 to 0.0012 | medium sand |
| Bolling Airforce Base, District of Columbia | 0.0006 to 0.0015 | fine sand |
| Patrick Airforce Base, Florida | 0.00026 to 0.007 | fine to coarse sand |
| Elmendorf Airforce Base, Alaska | 0.10 to 0.25 | organic silt and peat |
| Elmendorf Airforce Base, Alaska | 0.0007 to 0.008 | silty sand |
| Elmendorf Airforce Base, Alaska | 0.0017 to 0.0019 | silt with sand, gravel and clay (glacial till) |
| Elmendorf Airforce Base, Alaska | 0.00125 | medium sand to gravel |
| Truax Field, Madison, Wisconsin | <0.0006 to 0.0061 | medium fine to sand |
| King Salmon Airforce Base, Alaska | 0.00021 to 0.019 | medium fine to sand |
| Battle Creek ANGB, Michigan | 0.00029 to 0.073 | fine to coarse sand |
| Oconee River, Georgia | 0.0057 | sand |
| Oconee River, Georgia | 0.020 to 0.029 | silt |

Tables based on Mackay 1990; Wiedemeier et al., 1995b; Karickhoff 1981; and Environmental Science and Engineering, Inc., Amherst, NH)

**Table C-4 - Equilibrium Sorption**

Soil-Water Partition Coefficient, $k_d$

For non-ionic organic compounds the soil-water partition coefficient, $k_d$ ($cm^3/g$) can be estimated from the following correlation with the organic carbon content of the soil:

$$k_d = f_{oc}\, k_{oc} \qquad (f_{oc} \geq 0.001)$$

where $f_{oc}$ is the fraction of organic carbon in the soil (grams organic carbon per gram soil) and $k_{oc}$ is the organic carbon/water partition coefficient ($cm^3/g$). Published $k_{oc}$ values are available from several sources (e.g., Lyman et al., 1982; U.S. EPA Public Health Risk Evaluation Database; and the web site www.epa.gov/oerrpage/superfund/resources/soil/part_5.pdf). Alternatively, $k_{oc}$ can be estimated (Seth et al., 1999) from a correlation with the octanol/water partition coefficient, $k_{ow}$ ($cm^3/g$), for which extensive databases and reliable estimation methods exist (e.g., Hansch and Leo 1979; Lyman et al., 1982; and the above-referenced EPA web site):

$$k_{oc} \cong 0.35\, k_{ow}$$

The above correlation is subject to variation by a factor of 2.5 in either direction. The above EPA web site also contains a summary of reported $k_d$ values for several inorganic constituents.

**Table C-5 - Colloid Particle Sizes**

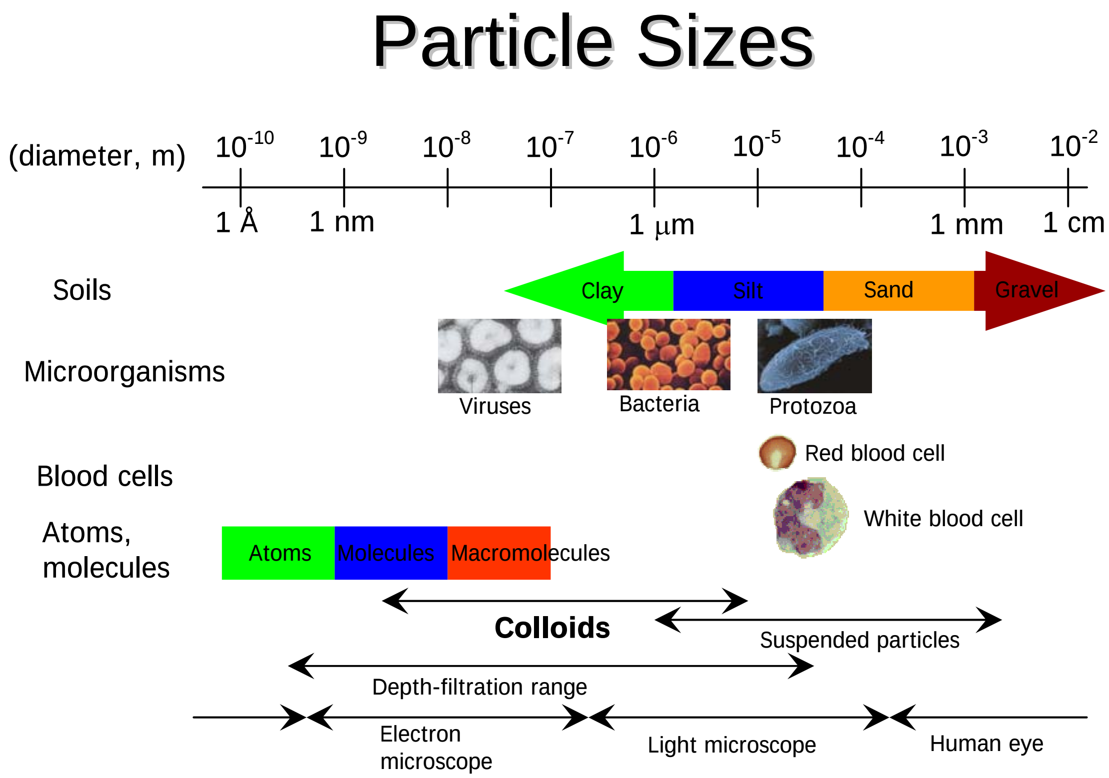


Based on DeNovio et al., 2004

## *Flow Model*

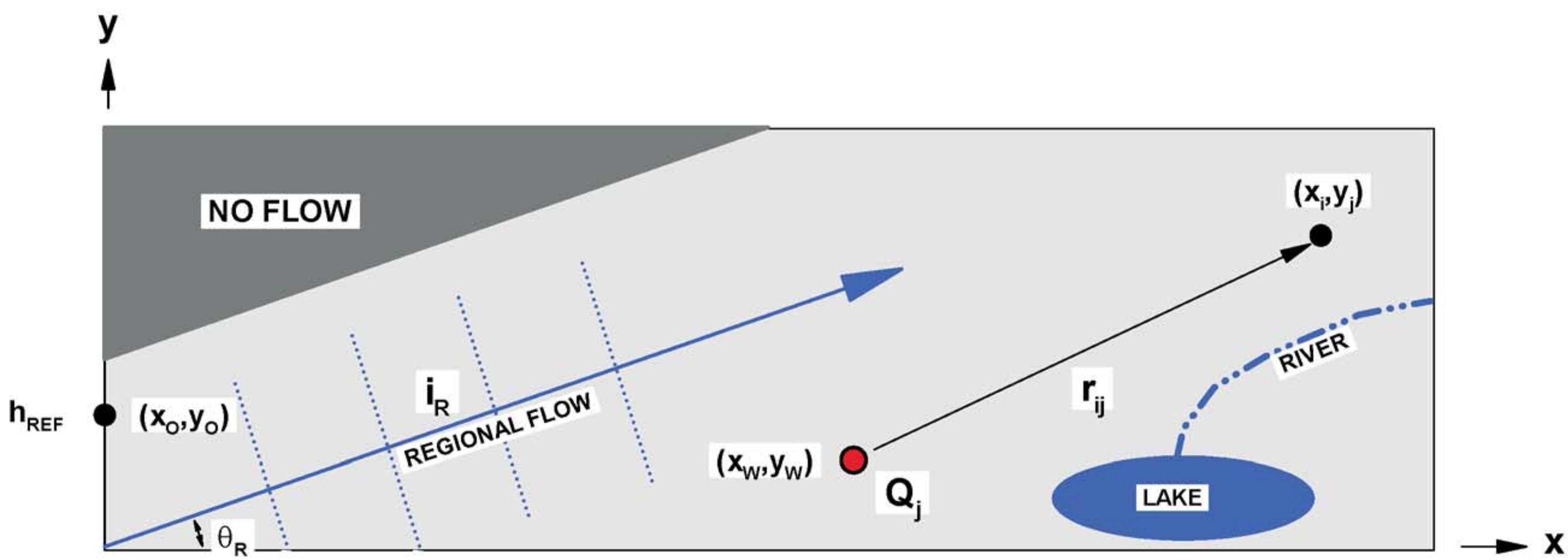


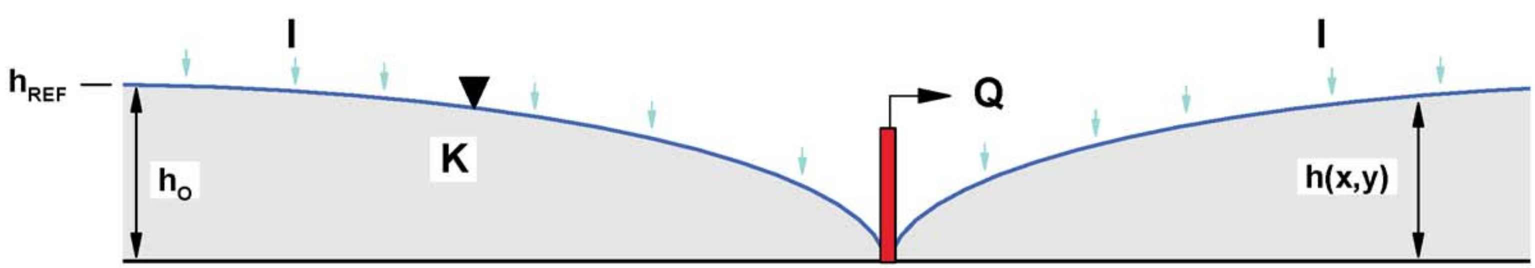


HARTCROWSER
2644-114 5/09
Figure C-1

EAL 04/15/09 2644114-AF.cdr

## *Concentration Interpolation at the Foot of the Characteristic Line*

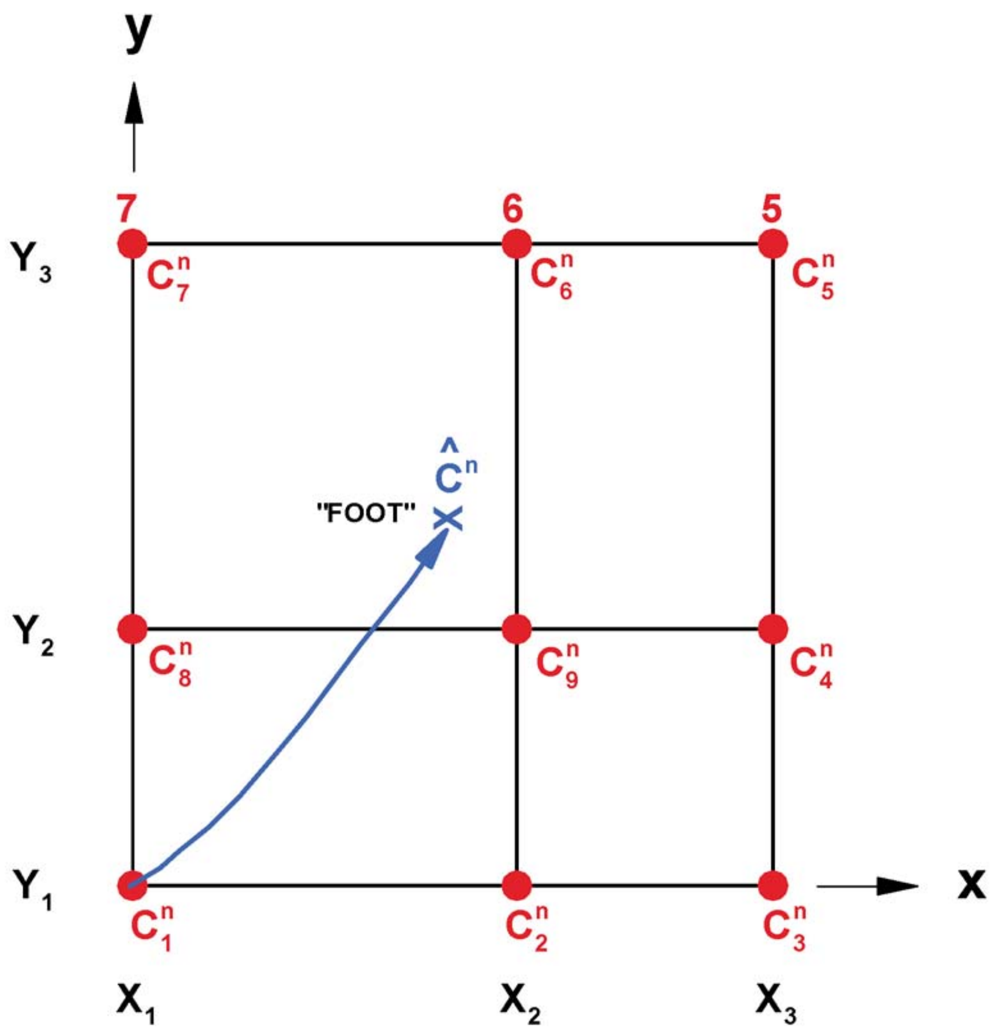


EAL 04/15/09 2644114-AG.cdr

HARTCROWSER
2644-114 5/09
Figure C-2

## *ADI Solution Approach*

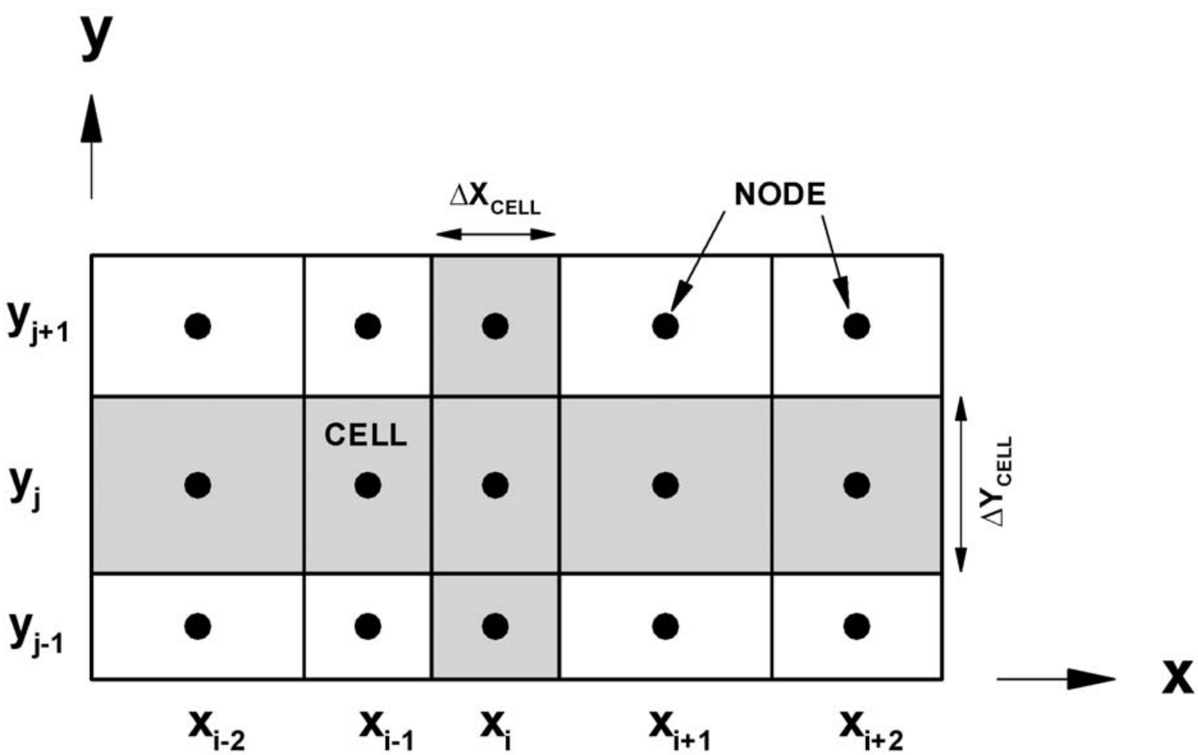


EAL 04/15/09 2644114-AH.cdr

HARTCROWSER
2644-114 5/09
*Figure C-3*

## *Test Problem 2 - RATLIM2D_PCB vs. COLFRAC*

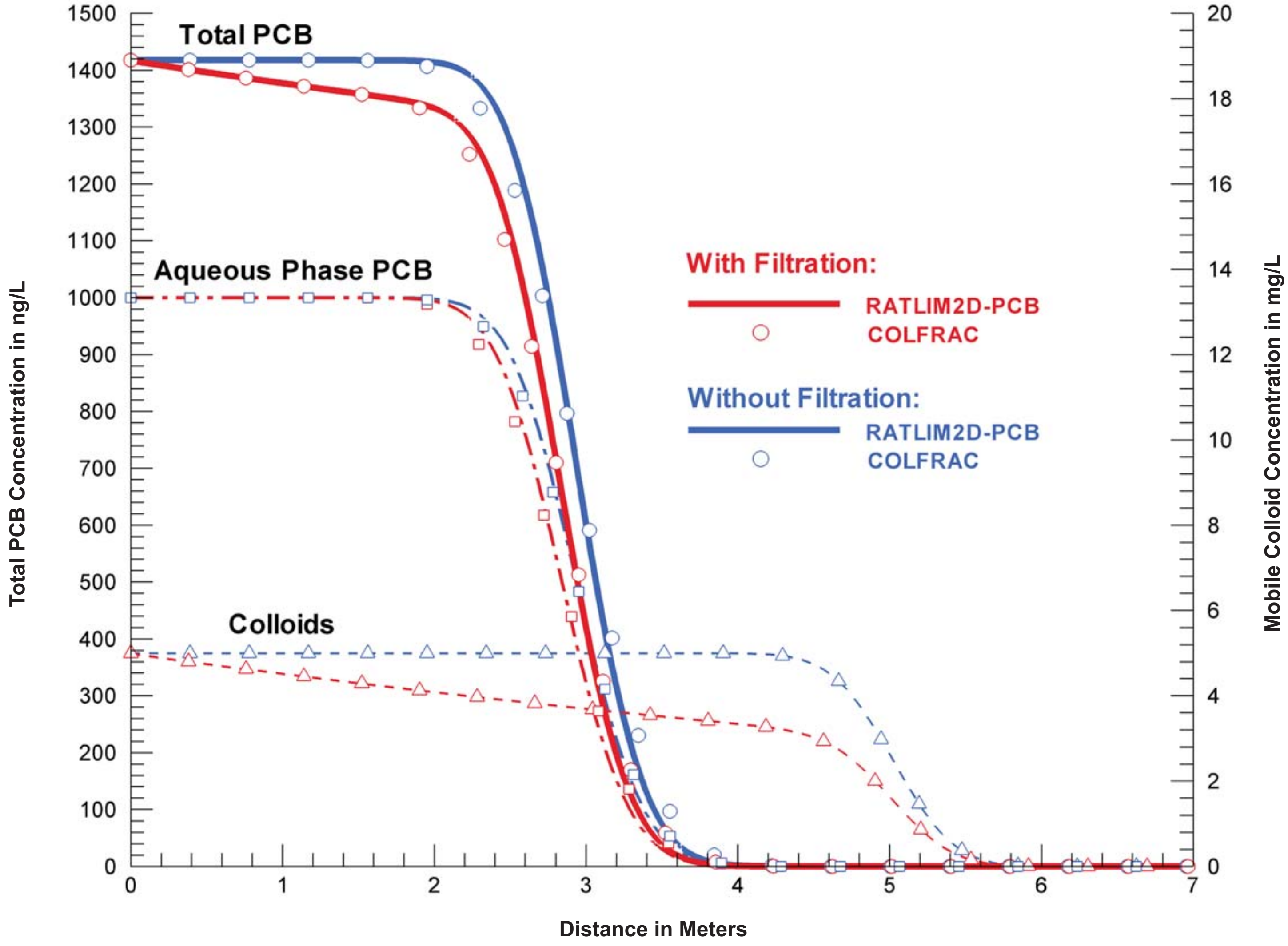


HARTCROWSER
2644-114 5/09
*Figure C-5*

## *Test Problem 3 - RATLIM2D_PCB vs. RBCA TIER 2 ANALYZER*

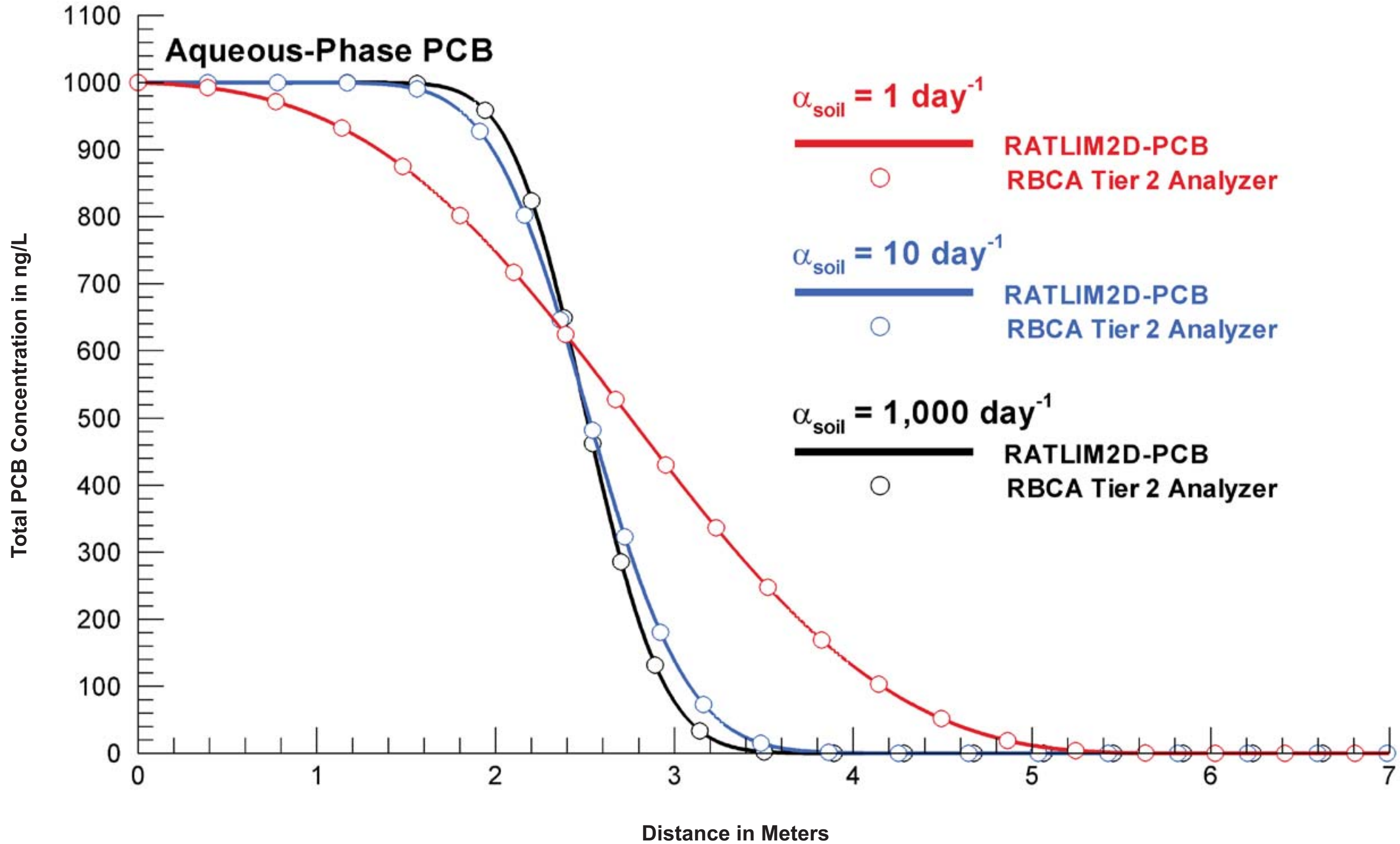


HARTCROWSER
2644-114 5/09
Figure C-6